Distributed Interference and Delay Aware Design for D2D Communication in Large Wireless Networks with Adaptive Interference Estimation

Sheng Huang, Ben Liang, *Senior Member, IEEE,* and Jiandong Li, *Senior Member, IEEE*

***Abstract*—We investigate distributed flow control and power allocation strategies for delay-aware Device-to-Device (D2D) communication underlaying large wireless networks, where D2D pairs reuse the resource blocks (RBs) of interior cellular users (CUEs). We consider a distributed D2D power allocation framework, where the D2D pairs individually attempt to maximize their own time-average throughput utility, while collectively guaranteeing the time-average coverage probability of CUEs in multiple cells. We design a novel method to compute the individual budget of interference from each D2D pair to CUEs based on stochastic geometry tools. Then, accounting for time-varying channel fading and dynamic D2D traffic arrival, we design a distributed interference-and-delay-aware (DIDA) flow control and power allocation strategy based on Lyapunov optimization and several interference estimation methods. We also analytically derive the performance bounds of D2D pairs and prove that the coverage probability of CUEs can be guaranteed regardless of the interference estimation error at D2D receivers. Finally, simulation results suggest that adaptive interference estimation methods are preferred and demonstrate that the DIDA strategy achieves substantial performance improvement against alternative strategies.**

I. Introduction

Device-to-device (D2D) communication enables two nearby users to communicate directly [1]–[3]. D2D communication in cellular networks can increase spectral efficiency and energy efficiency, reduce transmission delay, and help offload traffic from cellular networks [4], [5]. D2D communication can use either overlay or underlay spectrum access. In overlay spectrum access, D2D pairs and cellular users (CUEs) are allocated orthogonal Resource Blocks (RBs), while in underlay spectrum access, D2D pairs share RBs with CUEs. Commonly, underlay spectrum access is preferred because it can significantly enhance spectral efficiency. However, the coexistence of D2D pairs and CUEs in underlay spectrum access incurs both intra-tier and cross-tier interference. Therefore, we must appropriately balance the throughput demand of D2D pairs and the reliable communication of CUEs. Efficient interference management, e.g., through power allocation, is thus required for the successful coexistence of D2D pairs and CUEs, especially when the base stations (BSs), CUEs, and D2D pairs are randomly located.

Recently, extensive research on power allocation has aimed to maximize the spectral efficiency of D2D pairs under practical constraints in regular cellular networks [6]–[13]. As wireless networks become increasingly irregular, new power allocation strategies have also been developed to account for the inherent spatial randomness in large wireless networks [14]–[18], commonly using the Poisson Point Process (PPP) model. However, these works only concerned physical-layer performance without considering the queueing delay of D2D communication. Since many D2D applications are delay-sensitive [19], we should take queueing delay into account to design cross-layer strategies.

Some recent works [20]–[24] have investigated delay-aware resource allocation in D2D communication, considering both channel state information (CSI) and queue state information (QSI). Generally, CSI and QSI reveal the instantaneous transmission opportunities at the physical layer and the urgency of data flows, respectively. However, these works focused on designing centralized resource allocation algorithms, which not only require global CSI and global QSI but also incur high computation and communication complexity. In particular, the centralized algorithms proposed in these works are limited to a single-cell model that ignores the interference from CUEs and D2D transmitters in the other cells, which has limited practical applicability. Therefore, we focus on delay-aware D2D resource control in multiple cells. Note that, when considering multiple cells, a network-wide control framework would involve a prohibitively large amount of overhead for collecting the CSIs and QSIs and then informing the users of the centralized control decisions. Therefore, we prefer a distributed control framework that only requires each D2D pair to know its own CSI and QSI. In the absence of CSI, QSI, and power decision of other D2D pairs, each D2D pair individually makes its own control decision.

Distributed D2D resource allocation strategies face two main challenges. Firstly, the need to account for the intra- and inter-cell interference from all transmitters to CUEs, and the lack of a centralized record of CSI, make it difficult to quantify the impact of D2D communication on CUE performance. In this work, we guarantee the coverage probability of CUEs based on the statistical distribution of channel fading over the long term, rather than instantaneous CSI in each time slot. Secondly, under distributed strategies, the interference at D2D receivers in a time slot is an unknown random

This work has been supported by the Key Project of National Natural Science Foundation of China (Grant No. 91638202), the Key Project of National Natural Science Foundation of China (Grant No. 61231008), the National Natural Science Foundation of China (Grant No. 61072068), and the 111 Project (Grant No. B08038).

Sheng Huang, Jiandong Li are with the State Key Laboratory of Integrated Service Networks, Xidian University, Xi'an, Shaanxi, 710071, China (e-mail:shenghuang.xd@gmail.com, jdli@mail.xidian.edu.cn). Ben Liang is with the Department of Electrical and Computer Engineering, University of Toronto, Ontario, Canada (e-mail: liang@comm.utoronto.ca). Sheng Huang was a visiting student at the University of Toronto supported by the China Scholarship Council.

variable that depends on the power allocation decision of all D2D transmitters in the same time slot. Meanwhile, in order to efficiently control the power of D2D transmitters, it is necessary to predict the interference at each D2D receiver in a time slot. Generally, to predict the received interference level, one might either measure its received interference in the previous time slot or evaluate the interference level using more advanced estimation methods, but the effects of various interference estimation schemes on the interaction between CUEs and D2D pairs are not well understood.

In this paper, we focus on the design of *distributed* flow control and power allocation strategies for delay-aware D2D communication underlaying large wireless networks, which also take into account the interference created by the D2D pairs. Our main contribution is summarized as follows:

- In order to guarantee the coverage probability of CUEs in a distributed manner, we employ the tools of stochastic geometry to derive the time-average *individual interference budget* of each D2D pair, which represents the allowable transmit power level of D2D transmitters.
- Given the time-average individual D2D interference budget, we formulate a set of individual stochastic optimization problems for delay-aware D2D communication underlaying multiple cells, to maximize the time-average throughput utility of each D2D pair, subject to D2D queueing stability and the individual D2D interference budget.
- We design a distributed interference-and-delay-aware (DIDA) flow control and power allocation strategy based on Lyapunov optimization [25] and D2D received interference estimation. Although the power allocation problem is non-convex, we propose a low-complexity solution by utilizing some special mathematical structure of the objective function. Also, the queue length bound and throughput bound of D2D pairs using the DIDA strategy are analytically derived. In particular, we prove that the CUE coverage probability guarantee can be distributively satisfied regardless of whether the interference estimation by D2D receivers is exact.
- Four interference estimation methods for D2D pairs are designed and compared. These interference estimation methods facilitate simultaneous power allocation by D2D pairs in each time slot and alleviate the CSI sharing overhead. Extensive simulation results suggest that adaptive interference estimation methods are preferred to improve the D2D performance.
- We compare the DIDA strategy with Fixed and On-Off strategies by simulation. The Fixed strategy deterministically consumes the individual interference budget in each time slot. The On-Off strategy is modified from [16] with the satisfaction of individual interference budget. Simulation results indicate that the DIDA strategy with adaptive interference estimation obtains significant performance gain over these two strategies.

The rest of this paper is organized as follows. We discuss the related works in Section II. In Section III, we introduce the system model and the individual D2D optimization problem description. The individual D2D interference budgeting and the individual problem formulation are developed in Section IV. In Section V, the DIDA flow control and power allocation strategy are designed and analyzed. Four interference estimation methods are proposed and compared in Section VI. In Section VII, we verify the performance of DIDA strategy under the proposed interference estimation methods through simulation and comparison. We summarize this paper in Section VIII.

II. Related Work

The efficacy of D2D communication underlaying cellular networks is usually examined with three criteria: throughput, delay, and complexity.

Some prior works concerned the throughput metric (e.g., [6]–[13]). To maximize the sum-rate of a CUE-D2D match and satisfying cellular service constraints, joint resource sharing and power allocation methods were proposed in [6]–[9]. Based on interference pricing methods, two-step power allocation algorithms were proposed to maximize the throughput of D2D pairs while protecting the Quality of Service (QoS) of both D2D pairs and CUEs in [10] and to optimize the sum weighted utility of the system in [11]. Combining interference pricing methods and game theory, resource allocation approaches were designed to maximize the D2D sum-rate under the CUE rate constraints in [12] and to guarantee the QoS of both CUEs and D2D pairs in [13]. These works only concerned a single CUE-D2D match, a single cell, or regular cellular networks. In contrast, we investigate a multi-cell network topology where the locations of BSs, CUEs, and D2D transmitters are random.

Recently, power allocation strategies for D2D communication in random network models were studied and analyzed (e.g., [14]–[18]). The interference from underlay cognitive nodes was analyzed in [14] based on several transmit power allocation and receiver association schemes. In [15], the effect of the mode selection and power allocation of D2D communication on cellular network performance was investigated. To maximize the D2D sum rate, on-off power allocation was proposed and analyzed in [16] by characterizing the D2D transmission capacity and optimizing the on-off threshold of D2D pairs. Similarly, based on the conditional success probability of a typical D2D pair, SIR-aware access control was proposed in [17] to maximize the area spectral efficiency of D2D pairs. In [18], a distributed random access protocol was designed and analyzed to avoid packet collision of D2D pairs, which protects D2D receivers by creating exclusion regions. However, these works only designed deterministic or on-off power allocation schemes. In addition, none of these works consider flow control for delay-sensitive D2D applications.

Considering the trade-off between throughput and delay, delay-aware flow control and power allocation strategies have been designed for D2D communication underlaying cellular networks (e.g., [20]–[24]). Based on Markov decision processes and the Bellman-equation, a delay-aware resource allocation and power control algorithm was designed in [20] to minimize the average delay and average drop rate of D2D pairs; joint mode selection and resource allocation strategies

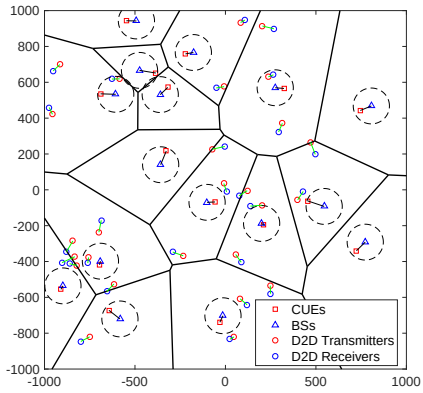

Fig. 1. An illustrated scenario of the system model.

were devised in [21], [22] to minimize the average weighted sum delay of both CUEs and D2D pairs subject to dropping probability constraints; dynamic power allocation for overlay D2D communication was proposed in [23] to minimize the weighted average transmit power and weighted average delay of D2D pairs. Based on the stochastic Lyapunov optimization theory, an on-line power allocation algorithm was proposed in [24] to address the trade-off between energy efficiency and delay in D2D communication underlaying cellular networks. Yet, these works focused on the design of centralized algorithms by collecting global CSI and QSI in a single cell. In contrast, we design distributed delay-aware flow control and power allocation strategies with low complexity for D2D communication underlaying large wireless networks.

A preliminary version of this work appeared in [26]. The current version adds detailed theoretical analysis of the DIDA strategy, four interference estimation methods for D2D pairs, and more substantial discussion and simulation results.

III. System Model

We consider a two-tier network with BSs, CUEs, and D2D pairs, as illustrated in Fig. 1. The locations of BSs, CUEs, and D2D transmitters follow independent PPPs $\Phi_{\mathcal{B}}$, $\Phi_{\mathcal{C}}$, and $\Phi_{\mathcal{D}}$ of density $\lambda_{\mathcal{B}}$, $\lambda_{\mathcal{C}}$, and $\lambda_{\mathcal{D}}$, respectively. Each CUE is associated with its nearest BS. A partial list of notations is given in Table I.

A. Spectrum Reuse and Channel Model

Within each cell, the CUEs are assigned different RBs, so that there is no intra-cell interference among them. To mitigate the inter-cell interference among CUEs, a standard fractional frequency reuse scheme is applied by dividing the CUEs into two groups, interior CUEs and edge CUEs. The interior CUEs of all cells share a part of the spectrum with reuse factor one, while the edge CUEs share a different part of the spectrum with lower reuse [27]. We assume that the spectrum allocation is pre-defined and focus on the analysis of interference over one given RB. We pick the one interior CUE using the given RB in every cell and denote these CUEs as the set $\Phi_{\mathcal{C}}^{\mathrm{RB}}$.

We consider sharing the uplink portion of cellular spectrum by D2D pairs. Since edge CUEs usually experience worse

TABLE I
Notation Table

Notation	Description
$\lambda_{\mathcal{B}}$, $\lambda_{\mathcal{C}}$, $\lambda_{\mathcal{D}}$	Density of PPPs $\Phi_{\mathcal{B}}$, $\Phi_{\mathcal{C}}$, and $\Phi_{\mathcal{D}}$ for BSs, CUEs, and D2D transmitters
R_F	Radius of an interior circle in the FFR scheme
$\Phi_{\mathcal{C}}^{\mathrm{RB}}$	Set of interior CUEs using a given RB
$r_{i,j}^{-\alpha}$, $r_{i,j}^{-\nu}$	Path-loss from transmitter i to receiver j for UE-to-BS channels and UE-to-UE channels
$g_{i,j}$	Channel fading from transmitter i to receiver j
ρ	Uplink received signal power target of CUEs
$P_n(t)$	Transmit power of D2D transmitter n
$A_n(t)$	Arrival traffic amount of D2D transmitter n
$\gamma_n(t)$	Admitted traffic amount of D2D transmitter n
$Q_n(t)$	Data queue length of D2D pair n
η	SINR threshold of interior CUEs
β	Coverage probability threshold of interior CUEs
$Z_n(t)$	Virtual power queue length of D2D pair n
ξ	Constant guard radius of the CGE method
$P(t)$	Approximated mean transmit power of D2D pairs
$d_{\hat{c},n}$, $d_{\hat{k},n}$	Distance from D2D receiver n to its nearest CUE and its nearest interfering D2D transmitter
$\tilde{I}_{\mathcal{C},n}(t)$, $\tilde{I}_{\mathcal{D},n}(t)$	Estimated mean aggregate interference from CUEs and D2D transmitters to D2D receiver n
$\bar{x}$	Time-average expectation of x
$\tilde{x}$	Approximated value of x
$\hat{x}$	A selected value within the domain of x
x^*	Optimal value within the domain of x

performance than interior CUEs, to protect the performance of edge CUEs, we assume D2D pairs reuse the RB allocated to the interior CUEs in $\Phi_{\mathcal{C}}^{\mathrm{RB}}$ and focus on the flow control and power allocation of D2D communication over the given RB. We define interior CUEs as those within the circle $B(\mathbf{x}_i, R_F)$ of radius R_F centered at their associated BS $\mathbf{x}_i$. An illustration of this D2D communication model is shown in Fig. 1.

Let $r_{i,j}$ be the distance between a transmitter i and a receiver j. We note that the path-loss exponents for UE-to-BS channels and UE-to-UE channels are usually different, where UE stands for either CUE, D2D transmitter, or D2D receiver. Therefore, we use path-loss models of $r_{i,j}^{-\alpha}$ and $r_{i,j}^{-\nu}$ for UE-to-BS channels and UE-to-UE channels, respectively. Further, we follow the conventional assumption that uplink power allocation adjusts for propagation losses [15], [28]. Specifically, the transmit power P_m of CUE m is based on channel-inversion power allocation of the form $P_m = \rho r_{m,m}^{\alpha}$, where ρ is the uplink received signal power target of CUEs. We define $\mathcal{P}(t) = \{P_n(t) | n \in \Phi_{\mathcal{D}}\}$ as the transmit power set of D2D transmitters in time slot t. Let $\mathcal{G}(t) = \{g_{i,j}(t) | i, j \in \Phi_{\mathcal{D}} \cup \Phi_{\mathcal{C}}^{\mathrm{RB}}\}$ be the channel gain set in time slot t under Rayleigh fading, where $g_{i,j}(t)$ represents small-scale fading from transmitter i to receiver j and is independently exponentially distributed with unit mean. Note that we use the subscript $(\cdot)_{i,i}$ to denote the transmission link from CUE i to its associated BS, or from D2D transmitter i to its own receiver.

The signal-to-interference-plus-noise-ratio (SINR) of BS m and D2D receiver n in time slot t are, respectively, given by

$$\mathrm{SINR}_m(t) = \frac{\rho g_{m,m}(t)}{I_{\mathcal{C},m}(t) + I_{\mathcal{D},m}(t) + \sigma^2}, \tag{1}$$

$$\text{SINR}_n(t) = \frac{P_n(t) r_{n,n}^{-\nu} g_{n,n}(t)}{I_{\mathcal{C},n}(t) + I_{\mathcal{D},n}(t) + \sigma^2}, \quad (2)$$

where $I_{\mathcal{C},m}(t) = \sum_{i \in \Phi_{\mathcal{C}}^{\text{RB}} \setminus \{m\}} \rho r_{i,i}^{\alpha} r_{i,m}^{-\alpha} g_{i,m}(t)$, $I_{\mathcal{D},m}(t) = \sum_{k \in \Phi_{\mathcal{D}}} P_k(t) r_{k,m}^{-\alpha} g_{k,m}(t)$, $I_{\mathcal{C},n}(t) = \sum_{i \in \Phi_{\mathcal{C}}^{\text{RB}}} \rho r_{i,i}^{\alpha} r_{i,n}^{-\nu} g_{i,n}(t)$, $I_{\mathcal{D},n}(t) = \sum_{k \in \Phi_{\mathcal{D}} \setminus \{n\}} P_k(t) r_{k,n}^{-\nu} g_{k,n}(t)$, and σ^2 is the noise power.

B. Traffic Models and Data Queues

Since the CUEs and D2D pairs typically support different communication applications, we consider a saturated traffic model for CUEs and a dynamic traffic model for D2D pairs. The arrival traffic amount of D2D pair n in time slot t is defined as $A_n(t) \in [0, A_{\max}]$, where $A_{\max}$ represents the maximum arrival traffic amount. To limit the queueing delay of each D2D pair, a flow control scheme is applied and the admitted traffic amount $\gamma_n(t)$ is constrained by

$$\gamma_n(t) \in [0, A_n(t)], \forall n \in \Phi_{\mathcal{D}}, \forall t, \quad (3)$$

where the admitted traffic $\gamma_n(t)$ is input to a data queue at the end of time slot t for transmission.

Further, the transmission amount of D2D pair n in time slot t is

$$R_n(\mathcal{P}(t), \mathcal{G}(t)) = w\tau \log_2 \left(1 + \text{SINR}_n(t)\right), \forall n \in \Phi_{\mathcal{D}}, \quad (4)$$

where w is the spectrum bandwidth of a RB and τ is the duration of a time slot. Due to hardware limitation, the instantaneous transmit power $P_n(t)$ must be constrained by

$$P_n(t) \in [0, P_{\max}], \forall n \in \Phi_{\mathcal{D}}, \forall t, \quad (5)$$

where $P_{\max}$ is the maximum D2D transmit power.

Then, the data queue $Q_n(t)$ of D2D pair $n \in \Phi_{\mathcal{D}}$, with $Q_n(0) = 0$, can be expressed as

$$Q_n(t+1) = \max\{Q_n(t) - R_n(\mathcal{P}(t), \mathcal{G}(t)), 0\} + \gamma_n(t). \quad (6)$$

C. Coverage Probability Guarantee of Interior CUEs

We are interested in the effect of D2D communication on the coverage probability $\mathbb{P}(\text{SINR}_m(t) > \eta)$ of CUE $m, \forall m \in \Phi_{\mathcal{C}}^{\text{RB}}$, where η is a given SINR threshold. In particular, we define the coverage probability guarantee of interior CUEs as

$$\limsup_{T \to \infty} \frac{1}{T} \sum_{t=0}^{T-1} \ln \mathbb{P}\left(\text{SINR}_m(t) > \eta\right) \geq \ln \beta, \forall m \in \Phi_{\mathcal{C}}^{\text{RB}}, \quad (7)$$

where $\beta \in (0, 1]$ is the coverage probability threshold of interior CUEs. The coverage probability constraint (7) intuitively provides an acceptable uplink coverage probability for interior CUEs over the long term. The formulation of (7) is motivated by recent subjective experiments on user responses to delay distributions [29], which has shown that users prefer small frequently occurring delays over rarely occurring but long delays. The sum-log utility in (7) enforces proportional fairness in the time dimension for each CUE, which helps even out the fluctuation of uplink outage probability over time, hence reducing the occurrence of long delays.

D. D2D Optimization Problem

As stated in Section I, distributed strategies can alleviate the communication complexity of sharing CSI and QSI in multiple cells. Thus, we consider a distributed D2D resource control framework where each D2D pair *individually* operates flow control and power allocation based on its own CSI and QSI, while all D2D pairs *collectively* guarantee the performance of CUEs in multiple cells in the long term. Considering each D2D pair has its own throughput utility defined by $\psi_n(\gamma_n(t))$, the individual optimization problem for D2D pair n, $\forall n \in \Phi_{\mathcal{D}}$, is to control $\gamma_n(t)$ and $P_n(t)$ to selfishly maximize its own time-average throughput utility $\overline{\psi_n(\gamma_n)} = \limsup_{T \to \infty} \frac{1}{T} \sum_{t=0}^{T-1} \mathbb{E}\{\psi_n(\gamma_n(t))\}$, so that the following requirements are guaranteed:

- C1: Flow control constraint (3) is satisfied;
- C2: Power constraint (5) is satisfied;
- C3: Queue (6) is strongly stable;
- C4: CUE coverage probability requirement (7) is satisfied in a distributed manner.

To keep mathematical exposition simple, we assume that the utility function $\psi_n(\cdot)$ is continuously differentiable and concave and denote its derivative by $\psi_n'(\cdot)$. Based on the assumption, there exists $\psi_{n,\min}'$ and $\psi_{n,\max}'$, such that $\psi_n'(\gamma_n(t)) \in [\psi_{n,\min}', \psi_{n,\max}'], \forall \gamma_n(t) \in [0, A_{\max}]$.

Note that it is challenging to distributively satisfy constraint C4. The CUE coverage probability $\mathbb{P}(\text{SINR}_m(t) > \eta)$ of interior CUE m concerns the interference created by *all* CUEs and D2D transmitters sharing the same RB. It depends on many random quantities, including the distances $r_{i,m}, \forall i \in \Phi_{\mathcal{D}} \cup \Phi_{\mathcal{C}}^{\text{RB}}, \forall m \in \Phi_{\mathcal{C}}^{\text{RB}}$, the channel states $\mathcal{G}(t)$, and the power decisions $\mathcal{P}(t)$, which are mostly unavailable to individual D2D pairs.

IV. Individual Interference Budgeting

To satisfy constraint C4 under a distributed D2D power allocation framework, we derive an *individual interference budget* that each D2D pair may not exceed toward the CUEs. Then, based on the individual interference budget, we formulate a set of individual stochastic optimization problems for D2D pairs.

A. Individual D2D Interference Budgeting

The coverage probability of interior CUEs in $\Phi_{\mathcal{C}}^{\text{RB}}$ is affected by the interference from all out-of-cell CUEs in $\Phi_{\mathcal{C}}^{\text{RB}}$ and D2D pairs that share the same RB. In order to satisfy the CUE coverage probability guarantee (7) in a distributed manner, we first quantify the interference from all out-of-cell CUEs and then compute how much of the remaining allowance of interference may be shared among the D2D interferers under the distributed D2D power allocation framework.

We first restate the interference from all interfering CUEs to the typical BS $\mathbf{x}_m$ in slot t as

$$I_{\mathcal{C},m}(t) = \sum_{\mathbf{x}_i \in \Phi_{\mathcal{B}} \setminus \{\mathbf{x}_m\}} I_{\mathbf{y}_{\mathbf{x}_i}, \mathbf{x}_m}(t), \quad (8)$$

where $\mathbf{x}_i$ is the coordinate of BS $\mathbf{x}_i$, $\mathbf{y}_{\mathbf{x}_i}$ represents the interior CUE using the given RB located at $\mathbf{y}_i$ inside cell $\mathbf{x}_i$, and

$I_{\mathbf{y}_{\mathbf{x}_i},\mathbf{x}_m}(t)$ denotes the interference from CUE $\mathbf{y}_{\mathbf{x}_i}$ to BS $\mathbf{x}_m$, which is given by

$$I_{\mathbf{y}_{\mathbf{x}_i},\mathbf{x}_m}(t) = \frac{\rho|\mathbf{y}_i - \mathbf{x}_i|^\alpha}{|\mathbf{y}_i - \mathbf{x}_m|^\alpha} g_{\mathbf{y}_i,\mathbf{x}_m}(t) \mathbf{1}_{|\mathbf{y}_i-\mathbf{x}_i|<|\mathbf{y}_i-\mathbf{x}_m|}. \quad (9)$$

Note that we index the interior CUE $\mathbf{y}_{\mathbf{x}_i}$ by its associated BS $\mathbf{x}_i$ in the sum operation of (8)[1]. Furthermore, $\rho|\mathbf{y}_i - \mathbf{x}_i|^\alpha$ indicates the transmit power of CUE $\mathbf{y}_{\mathbf{x}_i}$, and $\mathbf{1}_{|\mathbf{y}_i-\mathbf{x}_i|<|\mathbf{y}_i-\mathbf{x}_m|}$ follows from the cell association scheme of CUEs, which indicates that the distance between a CUE and its associated BS is smaller than the distance between the CUE to another BS. The Laplace transform of $I_{\mathbf{y}_{\mathbf{x}_i},\mathbf{x}_m}(t)$ is thus computed as

$$\begin{aligned}
&\mathcal{L}_{I_{\mathbf{y}_{\mathbf{x}_i},\mathbf{x}_m}(t)}(s) = \mathbb{E}_{\mathbf{y}_i, g_{\mathbf{y}_i,\mathbf{x}_m}(t)}\left[e^{-sI_{\mathbf{y}_{\mathbf{x}_i},\mathbf{x}_m}(t)}\right] \\
&= \mathbb{E}_{\mathbf{y}_i}\left[\frac{1}{1 + s\rho|\mathbf{y}_i - \mathbf{x}_i|^\alpha |\mathbf{y}_i - \mathbf{x}_m|^{-\alpha} \mathbf{1}_{|\mathbf{y}_i-\mathbf{x}_i|<|\mathbf{y}_i-\mathbf{x}_m|}}\right] \\
&\overset{(a)}{=} \int_{B(\mathbf{x}_i,R_F)} \frac{(\pi R_F^2)^{-1}}{1 + s\rho\frac{|\mathbf{y}_i-\mathbf{x}_i|^\alpha}{|\mathbf{y}_i-\mathbf{x}_m|^\alpha}\mathbf{1}_{|\mathbf{y}_i-\mathbf{x}_i|<|\mathbf{y}_i-\mathbf{x}_m|}} d\mathbf{y}_i, \quad (10)
\end{aligned}$$

where (a) follows from a simplifying assumption that R_F is small enough such that the area of an interior circle does not go beyond the boundary of the corresponding cell, and we have used the fact that $|\mathbf{y}_i - \mathbf{x}_m|^2 = |\mathbf{x}_i - \mathbf{y}_i|^2 + |\mathbf{x}_i - \mathbf{x}_m|^2 - 2(\mathbf{x}_i - \mathbf{y}_i)\cdot(\mathbf{x}_i - \mathbf{x}_m)$.

Next, we derive the Laplace transform $\mathcal{L}_{I_{\mathcal{C},m}}(s)$ by applying the superposition-aggregation-superposition method developed in [28]. Note that the remaining random variable in (10) is $\mathbf{x}_i$. Hence, the interfering signal from CUE $\mathbf{y}_{\mathbf{x}_i}$ to BS $\mathbf{x}_m$ can be equivalently regarded as emission from one aggregation point at BS $\mathbf{x}_i$. Therefore, the overall interference from all out-of-cell CUEs $\mathbf{y}_{\mathbf{x}_i}, \forall \mathbf{x}_i \in \Phi_{\mathcal{B}} \setminus \{\mathbf{x}_m\}$ using the given RB can be represented by a function of these aggregation points $\mathbf{x}_i$. The Laplace transform $\mathcal{L}_{I_{\mathcal{C},m}}(s)$ is thus derived as

$$\begin{aligned}
\mathcal{L}_{I_{\mathcal{C},m}}(s) =& \mathbb{E}\Big[\prod_{\mathbf{x}_i\in\Phi_{\mathcal{B}}\setminus\{\mathbf{x}_m\}} e^{-sI_{\mathbf{y}_{\mathbf{x}_i},\mathbf{x}_m}}\Big] \\
\overset{(b)}{=}& \mathbb{E}\Big[\mathbb{E}\Big(\prod_{\mathbf{x}_i\in\Phi_{\mathcal{B}}\setminus\{\mathbf{x}_m\}} e^{-sI_{\mathbf{y}_{\mathbf{x}_i},\mathbf{x}_m}} \Big| \Phi_{\mathcal{B}}\Big)\Big] \quad (11) \\
\overset{(c)}{=}& \mathbb{E}\Big[\prod_{\mathbf{x}_i\in\Phi_{\mathcal{B}}\setminus\{\mathbf{x}_m\}} \mathcal{L}_{I_{\mathbf{y}_{\mathbf{x}_i},\mathbf{x}_m}}(s)\Big] \\
\overset{(d)}{=}& \exp\Bigg(-\lambda_{\mathcal{B}} 2\pi \int_0^\infty \Big(1 - \mathcal{L}_{I_{\mathbf{y}_{\mathbf{x}_i},\mathbf{x}_m}(t)}(s)\Big) \\
&\times |\mathbf{x}_i - \mathbf{x}_m|\, d|\mathbf{x}_i - \mathbf{x}_m|\Bigg),
\end{aligned}$$

where (b) follows from conditional expectation; (c) holds because, given $\Phi_{\mathcal{B}}$, the interference signals from CUEs $\mathbf{y}_{\mathbf{x}_i}$ are independent with each other; and (d) follows from the generating functional of PPP $\Phi_{\mathcal{B}}$ [30]. Since $\mathcal{L}_{I_{\mathbf{y}_{\mathbf{x}_i},\mathbf{x}_m}(t)}(s)$ depends on $\mathbf{x}_m$ only through vector $(\mathbf{x}_i - \mathbf{x}_m)$ and the above integration is over vector $(\mathbf{x}_i - \mathbf{x}_m)$, (11) is not a function of $\mathbf{x}_m$. Hence, (11) applies to all CUEs in $\Phi_{\mathcal{C}}^{\mathrm{RB}}$ and we may relabel $\mathcal{L}_{I_{\mathcal{C},m}(t)}(s)$ as $\mathcal{L}_{I_{\mathcal{C}}(t)}(s)$.

[1]Since the CUE density is generally much larger than the BS density, each cell usually contains multiple interior CUEs and the non-existence of interior CUE in a cell is rare. The given RB is shared over all cells with reuse factor one and allocated to one interior CUE in each cell.

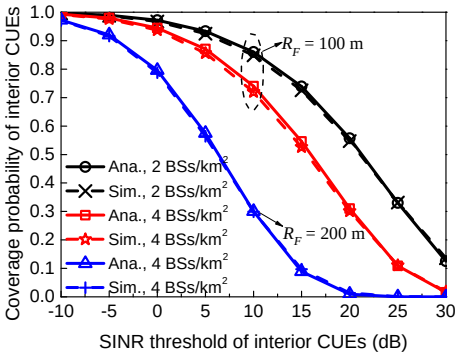

Fig. 2. Uplink coverage probability of interior CUEs in CUE-only scenarios with $\alpha = 3.75$ and $\rho = -50$ dBm.

In addition, under distributed power allocation strategies of D2D communication, the Laplace transform $\mathcal{L}_{I_{\mathcal{D},m}(t)}(s)$ of the total intra- and inter-cell interference $I_{\mathcal{D},m}(t)$ from D2D transmitters to the typical BS $\mathbf{x}_m$ in time slot t can be derived [16] in terms of $P_n(t)$ as

$$\mathcal{L}_{I_{\mathcal{D},m}(t)}(s) = \exp\left(-\frac{s^{\frac{2}{\alpha}}\pi\lambda_{\mathcal{D}}}{\mathrm{sinc}(\frac{2}{\alpha})}\mathbb{E}_{P_n}\left[P_n(t)^{\frac{2}{\alpha}}\right]\right), \quad (12)$$

where $\mathbb{E}_{P_n}[\cdot]$ is with respect to the unknown CSI and QSI for distributed delay-aware power allocation strategies. Since (12) does not depend on $\mathbf{x}_m$, we may relabel $\mathcal{L}_{I_{\mathcal{D},m}(t)}(s)$ as $\mathcal{L}_{I_{\mathcal{D}}(t)}(s)$.

Then, the uplink coverage probability of the interior CUE m in time slot t is derived as

$$\begin{aligned}
&\mathbb{P}\left(\mathrm{SINR}_m(t) > \eta\right) = \mathbb{P}\left(\frac{\rho g_{m,m}(t)}{I_{\mathcal{C},m}(t) + I_{\mathcal{D},m}(t) + \sigma^2} > \eta\right) \\
&= e^{-\frac{\eta\sigma^2}{\rho}} \mathcal{L}_{I_{\mathcal{C}}(t)}\left(\frac{\eta}{\rho}\right) \mathcal{L}_{I_{\mathcal{D}}(t)}\left(\frac{\eta}{\rho}\right). \quad (13)
\end{aligned}$$

Substituting (13) into (7), the CUE coverage probability requirement (7) is restated as

$$\limsup_{T\to\infty} \frac{1}{T}\sum_{t=0}^{T-1} \ln\left(U \exp\left(-S\mathbb{E}_{P_n}[P_n(t)^{\frac{2}{\alpha}}]\right)\right) \geq \ln\beta, \quad (14)$$

where $U = e^{-\frac{\eta\sigma^2}{\rho}} \mathcal{L}_{I_{\mathcal{C}}(t)}(\frac{\eta}{\rho})$ and $S = \frac{\pi\lambda_{\mathcal{D}}}{\mathrm{sinc}(\frac{2}{\alpha})}(\frac{\eta}{\rho})^{\frac{2}{\alpha}}$. With further manipulations, the CUE coverage probability requirement (14) is equivalently transformed into the following constraint on the time-average expectation of D2D transmit power:

$$\limsup_{T\to\infty} \frac{1}{T}\sum_{t=0}^{T-1} \mathbb{E}_{P_n}\left[P_n(t)^{\frac{2}{\alpha}}\right] \leq \frac{\ln U - \ln\beta}{S}, \forall n \in \Phi_D, \quad (15)$$

which acts as a time-average individual interference budget of each D2D pair to guarantee the coverage probability of CUEs. Note that (15) implies that D2D communication should only reuse the spectrum of those interior CUEs with $U > \beta$.

Remark 1: As the simplifying assumption in (10) affects the precision of $\mathcal{L}_{I_{\mathcal{C}}(t)}(\frac{\eta}{\rho})$, we verify that it gives tight approximations through simulation. Fig. 2 illustrates the uplink CUE coverage probability in CUE-only scenarios where no D2D

pairs are active, which is given by U as defined below (14). We observe that the computed U is accurate, which validated the tightness of $\mathcal{L}_{I_{\mathcal{C}}(t)}(\frac{\eta}{\rho})$. Similar results with other parameter settings are also observed but are omitted to avoid redundancy.

B. Individual D2D Optimization Problem Formulation

In reality, the individual interference budget $\frac{\ln U - \ln \beta}{S}$ may be calculated and broadcast by BSs to each D2D pair at the initial stage. In order to use the licensed spectrum, each D2D pair must obey the individual interference budget in its power allocation stage. Thus, each D2D pair selfishly maximizes its time-average throughput utility while satisfying the queueing stability of D2D communication and individual interference budget. Based on the problem description in Section III-D and treating the interference from CUEs and other D2D transmitters as noise, we formulate the individual delay-aware design problem of D2D pair n, $\forall n \in \Phi_{\mathcal{D}}$, as

$$\mathbf{P1}: \max_{\gamma_n(t), P_n(t)} \quad \overline{\psi_n(\gamma_n)} \tag{16}$$

$$s.t. \quad \bar{Q}_n < \infty, \tag{17}$$
$$(3), (5), (15),$$

where $\bar{Q}_n = \limsup_{T\to\infty} \frac{1}{T} \sum_{t=0}^{T-1} \mathbb{E}\{Q_n(t)\}$. According to the strong stability definition [25, Definition 2.7], the satisfaction of (17), i.e., finite average backlog, implies that the data queue $Q_n(t)$ is strongly stable.

Remark 2:

- Solving $\mathbf{P1}$ is challenging due to its stochastic nature and the constraint (15). Although the Lyapunov optimization approach [25] can be used to transform $\mathbf{P1}$ into a series of per-slot optimization problems, the time-average constraint (15) leads to a non-convex per-slot power allocation problem.
- In the absence of CSI and power decision sharing in a time slot t, the interference term $I_n(t) \triangleq I_{\mathcal{C},n}(t) + I_{\mathcal{D},n}(t)$ inside the $R_n(\mathcal{P}(t), \mathcal{G}(t))$ expression, as defined in (4), is an unknown random variable before the power allocation decision of D2D pairs in the time slot t is executed. Therefore, to solve problem $\mathbf{P1}$ at each D2D pair individually, the capability of interference estimation is required by D2D pairs. Under the distributed D2D power allocation framework, the need for sharing CSI and QSI is substantially reduced, e.g., the channel gain set $\mathcal{G}(t)$ in time slot t is not needed.
- Note that our problem formulation is based on the distributed power control framework in Section III-D, which limits the control information that can be used for resource control. The CUEs and D2D pairs do not need to share location, channel state, or queue state information, which implies that the individual interference budget (15) does not require the instantaneous CSI of interfering links from out-of-cell CUEs and D2D transmitters to BSs. In this case, we evaluate the impact of D2D communication on CUE performance based on the time-average expectation of D2D transmit power. Note that the parameters ρ, η, R_F, and β in (15) can be determined by the operator.

V. Distributed Interference-and-Delay-Aware Flow Control and Power Allocation Design

To solve problem $\mathbf{P1}$ by each D2D pair respectively, we employ Lyapunov optimization approach [25] and D2D interference estimation to design a distributed flow control and power allocation strategy. Further, we analytically quantify the performance bounds of each D2D pair.

A. Separable Problem Reformulation

Based on the Lyapunov optimization approach [25], we transform constraints (15) and (17) into queueing stability constraints and construct a separable problem reformulation.

We define a virtual power queue for D2D transmitter n as

$$Z_n(t+1) = \max\{Z_n(t) + P_n(t)^{\frac{2}{\alpha}} - \frac{\ln U - \ln \beta}{S}, 0\}, \tag{18}$$

with $Z_n(0) = 0$. According to the *Rate Stability* Theorem [25, Theorem 2.5], satisfying constraints (15) and (17) are equivalent to maintaining the stability of (18) and (6), respectively.

For all t and all control decisions $(\gamma_n(t), P_n(t))$, as in [25], we assume the following necessary but practical upper-bound conditions,

$$\mathbb{E}\{\gamma_n(t)^2\} \le A_{\max}^2, \quad \forall n \in \Phi_{\mathcal{D}}, \tag{19}$$

$$\mathbb{E}\{R_n(\mathcal{P}(t), \mathcal{G}(t))^2\} \le R_{\max}^2, \quad \forall n \in \Phi_{\mathcal{D}}, \tag{20}$$

$$\mathbb{E}\Big\{(P_n(t)^{\frac{2}{\alpha}} - \frac{\ln U - \ln \beta}{S})^2\Big\} \le P_{\max}^{\frac{4}{\alpha^2}}, \quad \forall n \in \Phi_{\mathcal{D}}, \tag{21}$$

hold for some finite constant parameters $A_{\max}$, $R_{\max}$, and $P_{\max}$. These assumptions are reasonable because arrival traffic amount, transmission amount, and transmit power are generally bounded according to the type of services, modulation and coding schemes, and regulatory power limits.

We then define a Lyapunov function and one-slot conditional Lyapunov drift, given by

$$L(\mathbf{\Theta}_n(t)) = \frac{1}{2} Q_n(t)^2 + \frac{1}{2} Z_n(t)^2, \tag{22}$$

$$\Delta(\mathbf{\Theta}_n(t)) = \mathbb{E}\{L(\mathbf{\Theta}_n(t+1)) - L(\mathbf{\Theta}_n(t)) | \mathbf{\Theta}_n(t)\}. \tag{23}$$

We further construct a Lyapunov *drift-plus-penalty* function [25] with respect to the objective (16) and the constraints (15) and (17) as follows:

$$\begin{aligned} &\Delta(\mathbf{\Theta}_n(t)) - V\mathbb{E}\{\psi_n(\gamma_n(t)) | \mathbf{\Theta}_n(t)\} \\ &\le B - V\mathbb{E}\{\psi_n(\gamma_n(t)) | \mathbf{\Theta}_n(t)\} \\ &+ Q_n(t)\mathbb{E}\left\{\gamma_n(t) - R_n(\mathcal{P}(t), \mathcal{G}(t)) | \mathbf{\Theta}_n(t)\right\} \\ &+ Z_n(t)\mathbb{E}\Big\{P_n(t)^{\frac{2}{\alpha}} - \frac{\ln U - \ln \beta}{S} \Big| \mathbf{\Theta}_n(t)\Big\}, \forall n \in \Phi_{\mathcal{D}}, \end{aligned} \tag{24}$$

where the right-hand side above is obtained by adopting the general derivation in [25], V is a control parameter, and B is a positive constant given by $B \triangleq \frac{1}{2}(A_{\max}^2 + R_{\max}^2 + P_{\max}^{\frac{4}{\alpha^2}})$.

Following the general Lyapunov optimization approach, we transform problem $\mathbf{P1}$ into minimizing the upper bound (24) subject to (3) and (5), with V as a tuning parameter that determines the tradeoff between the throughput and queueing delay of D2D pairs. Specifically, in each time slot t, every D2D pair n, $\forall n \in \Phi_{\mathcal{D}}$, makes a flow control and power allocation decision $(\gamma_n(t), P_n(t))$ by observing its current QSI $\mathbf{\Theta}_n(t)$

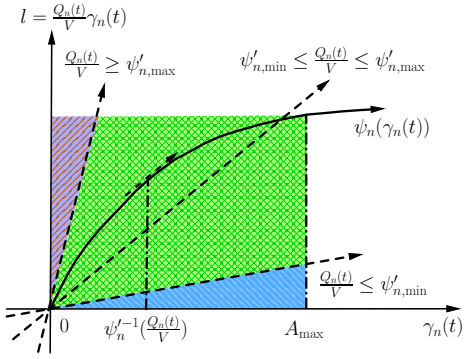

Fig. 3. Illustration of the definition of function $f_n(\frac{Q_n(t)}{V})$.

and its instantaneous CSI $g_{n,n}(t)$, and solving the following two independent optimization problems:

$$\mathbf{P2}: \quad \min_{\gamma_n(t)} \quad Q_n(t)\gamma_n(t) - V\psi_n(\gamma_n(t)) \qquad (25)$$
$$s.t. \quad (3),$$

which is a distributed flow control problem on $\gamma_n(t)$, and

$$\mathbf{P3}: \quad \min_{P_n(t)} \quad Z_n(t)P_n(t)^{\frac{2}{\alpha}} - Q_n(t)R_n(\mathcal{P}(t),\mathcal{G}(t)) \qquad (26)$$
$$s.t. \quad (5),$$

which is a distributed power allocation problem on $P_n(t)$. Note that, unlike standard Lyapunov optimization, when D2D pair n makes its power allocation decision in time slot t, the interference term $I_n(t)$ inside $R_n(\mathcal{P}(t),\mathcal{G}(t))$ is an unknown random variable that depends on the decision of other D2D pairs in the same time slot.

We next present the proposed distributed flow control method for each D2D pair based on its own QSI, and distributed power allocation method for each D2D pair based on interference estimation and its own CSI and QSI.

B. DIDA Flow Control

The optimal solution $\gamma_n^*(t)$ of $\mathbf{P2}$ is easily decided by

$$\gamma_n^*(t) = \max\left\{\min\left\{f_n\left(\frac{Q_n(t)}{V}\right), A_n(t)\right\}, 0\right\}, \qquad (27)$$

with

$$f_n\left(\frac{Q_n(t)}{V}\right) = \begin{cases} A_{\max}, & \text{if } \frac{Q_n(t)}{V}\in[0,\psi'_{n,\min}), \\ \psi'^{-1}_n(\frac{Q_n(t)}{V}), & \text{if } \frac{Q_n(t)}{V}\in[\psi'_{n,\min},\psi'_{n,\max}], \\ 0, & \text{if } \frac{Q_n(t)}{V}\in(\psi'_{n,\max},+\infty), \end{cases} \qquad (28)$$

where $\psi'^{-1}_n(\cdot)$ is the inverse function of $\psi'_n(\cdot)$.

Remark 3:

- $Q_n(t)$ reflects the link congestion level of D2D pair n in time slot t. The variable V can be viewed as a control parameter of data dropping to limit queueing delay of D2D pairs. As illustrated in Fig. 3, the definition of function $f_n(\frac{Q_n(t)}{V})$ follows from the assumption that utility function $\psi_n(\cdot)$ is continuously differentiable and concave with $\psi'_n(0)=\psi'_{n,\max}$ and $\psi'_n(A_{\max})=\psi'_{n,\min}$. In addition, $\gamma_n^*(t)$ is the admitted traffic amount in time slot t, which further affects the data queue length.
- The rationale of (27) is to balance the tradeoff between throughput and delay. We use separate $A_n(t)$ for the traffic generation amount and $\gamma_n(t)$ for the admitted traffic amount to allow more flexible modeling of any system. Taking video adaptation [31] as an example, a video stream generates a traffic amount $A_n(t)$ that consists of one base layer and several enhancement layers. In order to limit the queueing delay, the transmitter may control the admitted traffic amount $\gamma_n(t)$ by discarding packets from the higher enhancement layers. In practical implementation, if the admitted traffic amount $\gamma_n(t)$ is smaller than the data generation amount $A_n(t)$, the data generator may eventually choose to reduce the data generation amount $A_n(t)$.

C. DIDA Power Allocation

In order to achieve distributed simultaneous power allocation of the D2D pairs, we must estimate the received interference power of each D2D receiver in time slot t to evaluate the transmission amount $R_n(\mathcal{P}(t),\mathcal{G}(t))$. Since the received interference power at each D2D receiver depends on the dynamic power allocation decision of all other D2D pairs, it changes over time and cannot be exactly measured before the power allocation decision is executed. Therefore, in each time slot, an estimation scheme is required to predict the interference that the D2D receiver will experience, in order to perform power allocation in the same time slot.

Four interference estimation methods will be presented in Section VI. However, the proposed DIDA strategy is compatible with any interference estimation method. Although the estimated interference is inexact, we will show in Section V-D that the individual D2D interference budget (15) and hence the CUE coverage probability guarantee (7) are always satisfied.

Let $\tilde{I}_{\mathcal{C},n}(t)$ and $\tilde{I}_{\mathcal{D},n}(t)$ be the estimated interference at D2D receiver n from the CUEs and interfering D2D transmitters, respectively. We define the approximated transmission amount of D2D pair n as

$$\tilde{R}_n(P_n(t),g_{n,n}(t)) \triangleq w\tau\log_2\left(1+\frac{P_n(t)r_{n,n}^{-\nu}g_{n,n}(t)}{\tilde{I}_{\mathcal{C},n}(t)+\tilde{I}_{\mathcal{D},n}(t)+\sigma^2}\right). \qquad (29)$$

We then replace problem $\mathbf{P3}$ by

$$\mathbf{P4}: \quad \min_{P_n(t)} Z_n(t)P_n(t)^{\frac{2}{\alpha}} - Q_n(t)\tilde{R}_n(P_n(t),g_{n,n}(t)) \qquad (30)$$
$$s.t. \ (5).$$

Note that $\mathbf{P4}$ is still a non-convex optimization problem. Nevertheless, we next propose a low-complexity algorithm to optimally solve problem $\mathbf{P4}$ by analyzing the mathematical structure of objective (30). Firstly, we rewrite (30) as

$$X(P_n(t)) = Z_n(t)P_n(t)^{\frac{2}{\alpha}} - J_n^t\log_2(1+K_n^tP_n(t)), \qquad (31)$$

where $J_n^t \triangleq Q_n(t)w\tau$ and $K_n^t \triangleq r_{n,n}^{-\nu}g_{n,n}(t)/(\tilde{I}_{\mathcal{C},n}(t)+\tilde{I}_{\mathcal{D},n}(t)+\sigma^2)$ are constant in time slot t. The derivative of

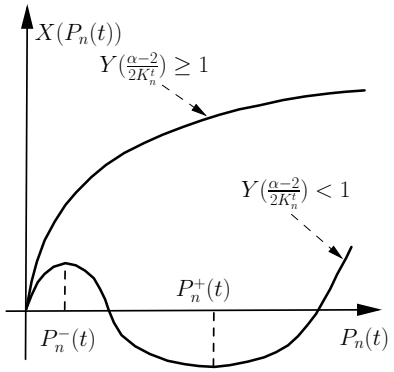

Fig. 4. Illustration of $X(P_n(t))$ with different values of $Y(\frac{\alpha-2}{2K_n^t})$.

$X(P_n(t))$ relative to $P_n(t)$ is given by

$$X'(P_n(t)) = \frac{2Z_n(t)}{\alpha} P_n(t)^{\frac{2}{\alpha}-1} - \frac{J_n^t K_n^t}{(1+K_n^t P_n(t))\ln 2}. \quad (32)$$

Dividing the first term of (32) by the second term of (32), we define $Y(P_n(t))$ and its derivative $Y'(P_n(t))$ relative to $P_n(t)$ as

$$Y(P_n(t)) = \frac{Z_n(t) 2\ln 2}{\alpha J_n^t K_n^t} \cdot \left(P_n(t)^{\frac{2}{\alpha}-1} + K_n^t P_n(t)^{\frac{2}{\alpha}} \right), \quad (33)$$

$$Y'(P_n(t)) = \frac{Z_n(t) 2\ln 2\,(2-\alpha+2K_n^t P_n(t))}{\alpha^2 J_n^t K_n^t P_n(t)^{2-\frac{2}{\alpha}}}. \quad (34)$$

We observe that, since the path-loss exponent α is normally larger than two,

$$Y'(P_n(t)) \begin{cases} < 0, & \forall P_n(t) \in \left[0, \frac{\alpha-2}{2K_n^t}\right), \\ > 0, & \forall P_n(t) \in \left(\frac{\alpha-2}{2K_n^t}, \infty\right). \end{cases} \quad (35)$$

Hence, $Y(P_n(t))$ is a quasiconvex function with $Y(0) = \infty$. Let $\tilde{P}_n^*(t)$, $\forall n \in \Phi_{\mathcal{D}}$, be the optimal power decision of $\mathbf{P4}$. If $Y(\frac{\alpha-2}{2K_n^t}) \geq 1$, then $X'(P_n(t)) \geq 0$ and $\tilde{P}_n^*(t) = 0$. Otherwise, if $Y(\frac{\alpha-2}{2K_n^t}) < 1$, we define $P_n^-(t)$ and $P_n^+(t)$ as the solutions to $Y(P_n(t)) = 1$ with $P_n^-(t) < P_n^+(t)$ and find that

$$X'(P_n(t)) \begin{cases} \geq 0, & \forall P_n(t) \in [0, P_n^-(t)] \cup [P_n^+(t), \infty), \\ \leq 0, & \forall P_n(t) \in [P_n^-(t), P_n^+(t)]. \end{cases} \quad (36)$$

Namely, if $Y(\frac{\alpha-2}{2K_n^t}) < 1$, $X(P_n(t))$ increases initially on $[0, P_n^-(t)]$, then decreases on $[P_n^-(t), P_n^+(t)]$, and increases again on $[P_n^+(t), \infty)$. Two illustrations of $X(P_n(t))$ are shown in Fig. 4. Consequently, $\tilde{P}_n^*(t)$ is determined by

$$\tilde{P}_n^*(t) = \begin{cases} \hat{P}_n(t), & \text{if } Y(\frac{\alpha-2}{2K_n^t}) < 1 \text{ and } X(\hat{P}_n(t)) < 0, \\ 0, & \text{otherwise}, \end{cases} \quad (37)$$

where

$$\hat{P}_n(t) \triangleq \min\{P_n^+(t), P_{\max}\} = \begin{cases} P_{\max}, & \text{if } \frac{\alpha-2}{2K_n^t} \geq P_{\max} \text{ or } Y(P_{\max}) \leq 1, \\ P_n^+(t), & \text{otherwise}. \end{cases} \quad (38)$$

Algorithm 1 DIDA flow control and power allocation strategy for D2D Pair n, $\forall n \in \Phi_{\mathcal{D}}$, in time slot t

1: **Interference budget (sent from BSs)**: $(\ln U - \ln \beta)/S$.
2: **Input**: $A_n(t)$, $Q_n(t)$, $Z_n(t)$, $g_{n,n}(t)$, $\tilde{I}_{\mathcal{C},n}(t)$, $\tilde{I}_{\mathcal{D},n}(t)$, σ^2.
3: Decide the admitted traffic amount $\gamma_n^*(t)$ by (27).
4: Decide the transmit power $\tilde{P}_n^*(t)$ according to (37).
5: Update queues $Q_n(t+1)$ and $Z_n(t+1)$ based on queueing laws (6) and (18).

D. Summary and Performance Bounds of the DIDA Strategy

1) Overall DIDA Description: We summarize the proposed DIDA flow control and power allocation strategy for each D2D pair in Algorithm 1.

2) Complexity Analysis of the DIDA Strategy: Given $P_n^+(t)$ for D2D pair n in time slot t, the flow control strategy (27) and power allocation strategy (37) are closed-form expressions with constant complexity. Note that $Y(P_n(t))$ is a quasiconvex function. According to (38), when $P_n^+(t)$ is required, $P_n^+(t)$ is located within $(\frac{\alpha-2}{2K_n^t}, P_{\max}]$ where $Y'(P_n(t)) > 0$. Thus, we could use the golden-section search method to obtain $P_n^+(t)$. Since $\frac{\alpha-2}{2K_n^t} > 0$, the maximum number of iteration steps required to ensure ε error tolerance is $\log_{0.618} \frac{\varepsilon}{P_{\max}}$. Further, for the case $\alpha = 4$, $P_n^+(t)$ can be obtained by solving a quadratic equation.

3) Performance Bounds of the DIDA Strategy: We analyze the queue length bounds and the strong stability of both data queues and virtual power queues in Theorem 1, and the time-average D2D throughput utility bound in Theorem 2.

Theorem 1 *Regardless of interference estimation error at D2D receivers, in each time slot t, the queue lengths of every data queue $Q_n(t)$ and every virtual power queue $Z_n(t)$ are, respectively, bounded by*

$$Q_n(t) \leq Q_{n,\max}, \quad Z_n(t) \leq Z_{n,\max}, \forall n \in \Phi_{\mathcal{D}}, \forall t. \quad (39)$$

where

$$Q_{n,\max} \triangleq V\psi'_{n,\max} + A_{\max}, \quad (40)$$

$$Z_{n,\max} \triangleq \frac{SR_{\max}(V\psi'_{n,\max} + A_{\max})}{(\ln U - \ln \beta)} + P_{\max}^{\frac{2}{\alpha}} - \frac{\ln U - \ln \beta}{S}. \quad (41)$$

As a result, the D2D queueing stability constraint (17) and the D2D individual interference budget (15) are satisfied.

Proof: See Appendix A. ■

Theorem 2 *Let $\{I_n(t)\}_{t=0}^{\infty}$ be the actual experienced interference of D2D receiver n. Denote $\mu_n(t)$ as the error ratio of the interference estimation at D2D receiver n in time slot t, i.e., $\tilde{I}_{\mathcal{C},n}(t) + \tilde{I}_{\mathcal{D},n}(t) = \mu_n(t) I_n(t)$ with $\mu_n(t) > 0$. Suppose that $\mathcal{G}(t)$ is i.i.d. over time slots and that the system satisfies the upper-bound conditions (19)-(21), under the distributed power allocation framework of D2D pairs, the time-average throughput utility of D2D pair n is lower bounded by*

$$\overline{\psi_n(\gamma_n)} \geq \hat{\psi}_n^*(\gamma_n) - \psi'_{n,\max} w\tau \overline{|\log_2 \mu_n|} - \frac{B + A_{\max} w\tau \overline{|\log_2 \mu_n|}}{V}, \forall n \in \Phi_{\mathcal{D}} \quad (42)$$

where $\overline{|\log_2 \mu_n|} = \limsup_{T\to\infty} \frac{1}{T}\sum_{t=0}^{T-1} |\log_2 \mu_n(t)|$ *and* $\hat{\psi}_n^*(\gamma_n)$ *is the optimal throughput utility of D2D pair* n *under its experienced interference* $\{I_n(t)\}_{t=0}^{\infty}$.

Proof: See Appendix B. ■

Remark 4:

- The strong stability of data queues is derived from the QSI-based flow control decision (27) and the strong stability of virtual power queues is obtained because the input amount yielded by the DIDA power allocation strategy is less than zero when the power queue length is excessively large. These strong stability results are stronger compared with the mean rate stabilization obtained directly by the general *Min Drift-Plus-Penalty Algorithm* [25]. In addition, the finite data queue length implies finite queueing delay based on Little's theorem [32].
- The stabilization of both data queues (6) and virtual power queues (18) are irrelevant to the accuracy of interference estimation in the proposed DIDA strategy. Therefore, the interference estimation error of D2D receivers only impacts the performance of D2D pairs, and the proposed DIDA strategy always satisfies the time-average individual interference budget (15) of D2D pairs and the time-average coverage probability guarantee (7) of interior CUEs.
- By forcing V to be infinity, the DIDA strategy achieves a solution with bounded throughput loss, which is quantified by the error ratio of interference estimation. This is because the performance gap between the optimal solutions of $\mathbf{P3}$ and $\mathbf{P4}$ is bounded by the interference estimation error. Note that the experienced interference of each D2D receiver in a time slot cannot be exactly measured before the power allocation decision is executed. Thus, $\hat{\psi}_n^*(\gamma_n)$ acts as an analytical upper bound that cannot be achieved by realistic distributed strategies. Moreover, the proposed DIDA strategy can achieve a trade-off between $1-O(\frac{1}{V})$ throughput and $O(V)$ queueing delay.

VI. D2D Interference Estimation Methods

In the previous section, the proposed DIDA strategy requires an estimation of the interference from all transmitters to every D2D receiver in each time slot. We face the following four challenges: 1) channel fading varies dramatically in different time slots; 2) the location of each interior CUE is coupled with that of its associated BS; 3) the transmit powers of interfering D2D transmitters are unknown in advance due to distributed simultaneous power allocation of D2D pairs in each time slot; 4) because the path-loss law $r^{-\nu}$ in our analytical model has a singularity point at $r=0$, the mean aggregate interference of each D2D receiver diverges [33].

To overcome these challenges, we propose four interference estimation methods. Specifically, the interference estimation methods are designed based on guard zones [34], the Campbell's Theorem [30], and the path-loss law. We discuss their relative merits in Section VI-E.

- *Constant Guard Estimation (CGE)*: Each D2D receiver n approximates the mean transmit power of D2D transmitters and calculates the estimated mean aggregate interference outside a constant guard zone based on Campbell's Theorem [30].
- *Adaptive Guard Estimation (AGE)*: Each D2D receiver n adaptively creates two guard zones based on the distances from its nearest CUE and its nearest interfering D2D transmitter. After approximating the mean transmit power of D2D transmitters, the estimated mean aggregate interference is then calculated based on Campbell's Theorem [30] and the path-loss law.
- *Extended Adaptive Guard Estimation (EAGE)*: Based on the AGE method, each D2D receiver n also measures the transmit power of its nearest CUE and accurately computes the mean interference from its nearest CUE.
- *Previous Interference Approximation (PIA)*: Each D2D receiver n uses the received interference power in the previous time slot.

A. Constant Guard Estimation (CGE)

In the CGE method, the estimated mean aggregate interference $\tilde{I}_{\mathcal{C},n}(t)$ from CUEs to D2D receiver n, $\forall n \in \Phi_{\mathcal{D}}$, is computed outside a guard zone $B(o_n,\xi)$ centered at the location o_n of D2D receiver n with a small radius ξ, given by

$$\begin{aligned}\tilde{I}_{\mathcal{C},n}(t) &= \mathbb{E}\left[\sum_{c\in\Phi_{\mathcal{C}}^{\mathrm{RB}}} \rho r_{c,c}^{\alpha} r_{c,n}^{-\nu} g_{c,n}(t)\mathbf{1}(r_{c,n}>\xi)\right] \\ &\overset{(e)}{=} \mathbb{E}\left[\rho r_{c,c}^{\alpha}\right]\mathbb{E}\left[g_{c,n}(t)\right]\cdot 2\pi\lambda_{\mathcal{B}}\int_{\xi}^{\infty} x^{-\nu}x\mathrm{d}x \qquad (43)\\ &= \frac{2\rho(\pi\lambda_{\mathcal{B}})^{1-\frac{\alpha}{2}}}{1-\exp(-\pi\lambda_{\mathcal{B}}R_F^2)}\cdot\frac{\xi^{2-\nu}}{\nu-2}\gamma\left(1+\frac{\alpha}{2},\pi\lambda_{\mathcal{B}}R_F^2\right),\end{aligned}$$

where (e) follows from Campbell's Theorem [30] by approximating $\Phi_{\mathcal{C}}^{\mathrm{RB}}$ as a PPP of density $\lambda_{\mathcal{B}}$, and $\gamma(a,x) = \int_0^x t^{a-1}e^{-t}\mathrm{d}t$ is the lower incomplete gamma function.

In addition, by using the CGE method, the estimated mean aggregate interference $\tilde{I}_{\mathcal{D},n}(t)$ from interfering D2D transmitters to D2D receiver n is computed outside the guard zone $B(o_n,\xi)$. Since the power allocation of D2D pairs is conducted distributively in each time slot, the transmit power of interfering D2D transmitters is unknown before the power allocation decision is executed. To overcome this difficulty, we introduce a new parameter $\bar{P}(t)$ to approximate the mean transmit power of interfering D2D transmitters in time slot t and define it as

$$\bar{P}(t) = \left(\frac{\ln U - \ln\beta}{S}\right)^{\frac{\alpha}{2}}, \forall t, \qquad (44)$$

where $\frac{\ln U-\ln\beta}{S}$ is the right-hand side of (15). As shown in Appendix C, $\bar{P}(t)$ is a lower bound of the time-average mean transmit power of interfering D2D transmitters when all the virtual power queues are stable. Further, the estimated mean aggregate interference $\tilde{I}_{\mathcal{D},n}(t)$ from interfering D2D transmitters to D2D receiver n, $\forall n \in \Phi_{\mathcal{D}}$, is calculated by

Campbell's Theorem [30] as

$$\begin{aligned}\tilde{I}_{\mathcal{D},n}(t) &= \mathbb{E}\left[\sum_{k\in\Phi_{\mathcal{D}}\setminus\{n\}} \bar{P}(t) r_{k,n}^{-\nu} g_{k,n}(t) \mathbf{1}(r_{k,n}\geq \xi)\right] \\ &= 2\pi\lambda_{\mathcal{D}} \frac{\xi^{2-\nu}}{\nu-2}\left(\frac{\ln U - \ln\beta}{S}\right)^{\frac{\alpha}{2}}.\end{aligned} \tag{45}$$

B. Adaptive Guard Estimation (AGE)

In the AGE method, we assume that each D2D receiver is capable of measuring distances to the nearest CUE and the nearest interfering D2D transmitter. Let $r_{\hat{c},n}$ be the measured distance between D2D receiver n and its nearest CUE $\hat{c}$. We calculate $\tilde{I}_{\mathcal{C},n}(t)$ as follows:

$$\begin{aligned}\tilde{I}_{\mathcal{C},n}(t) =& \mathbb{E}\left[\sum_{c\in\Phi_{\mathcal{C}}^{\mathrm{RB}}} \rho r_{c,c}^{\alpha} r_{c,n}^{-\nu} g_{c,n}(t)\mathbf{1}(r_{c,n}>r_{\hat{c},n})\right] \\ &+ \mathbb{E}\left[\rho r_{\hat{c},\hat{c}}^{\alpha} r_{\hat{c},n}^{-\nu} g_{\hat{c},n}(t)\right] \\ \overset{(f)}{=}& \frac{\rho(\pi\lambda_{\mathcal{B}})^{-\frac{\alpha}{2}}}{1-\exp(-\pi\lambda_{\mathcal{B}}R_F^2)}\cdot\gamma\left(1+\frac{\alpha}{2},\pi\lambda_{\mathcal{B}}R_F^2\right) \\ &\times\left(2\pi\lambda_{\mathcal{B}}\frac{r_{\hat{c},n}^{2-\nu}}{\nu-2}+r_{\hat{c},n}^{-\nu}\right),\end{aligned} \tag{46}$$

where (f) follows from the Campbell's Theorem [30] by approximating $\Phi_{\mathcal{C}}^{\mathrm{RB}}$ as a PPP of density $\lambda_{\mathcal{B}}$. Specifically, the first term of (46) is the estimated mean aggregate interference from the CUEs outside the guard zone $B(o_n, r_{\hat{c},n})$ and the second term of (46) is the estimated mean interference from the nearest CUE $\hat{c}$ located at the boundary of the guard zone $B(o_n, r_{\hat{c},n})$.

Similarly, let $r_{\hat{k},n}$ be the measured distance between D2D receiver n and its nearest interfering D2D transmitter $\hat{k}$. We calculate $\tilde{I}_{\mathcal{D},n}(t)$ based on the guard zone $B(o_n, r_{\hat{k},n})$ as follows:

$$\begin{aligned}\tilde{I}_{\mathcal{D},n}(t) =& \mathbb{E}\left[\sum_{k\in\Phi_{\mathcal{D}}\setminus\{n\}} \bar{P}(t) r_{k,n}^{-\nu} g_{k,n}(t)\mathbf{1}(r_{k,n}\geq r_{\hat{k},n})\right] \\ &+ \mathbb{E}\left[\bar{P}(t) r_{\hat{k},n}^{-\nu} g_{\hat{k},n}(t)\right] \\ =& \left(\frac{\ln U-\ln\beta}{S}\right)^{\frac{\alpha}{2}}\cdot\left(2\pi\lambda_{\mathcal{D}}\frac{r_{\hat{k},n}^{2-\nu}}{\nu-2}+r_{\hat{k},n}^{-\nu}\right).\end{aligned} \tag{47}$$

To measure the distances to the nearest CUE and the nearest interfering D2D transmitter, we could apply [5] to design two applicable schemes: 1) a push scheme, where CUEs and D2D transmitters periodically broadcast their location information, e.g., positioning reference signals [35]; 2) a pull mechanism, where D2D receivers periodically request location information such as positioning reference signals [35] regarding discoverable CUEs and D2D transmitters. Based on either of these two schemes, every D2D receiver registers the location information of nearby users, updates a distance list periodically, and finds the nearest CUE and the nearest interfering D2D transmitter from the distance list.

C. Extended Adaptive Guard Estimation (EAGE)

In the EAGE method, the transmit power $\rho r_{\hat{c},\hat{c}}^{\alpha}$ of the nearest CUE $\hat{c}$ is also measured. Then, $\tilde{I}_{\mathcal{D},n}(t)$ is calculated in the same way as the AGE method, while $\tilde{I}_{\mathcal{C},n}(t)$ is calculated by

$$\begin{aligned}\tilde{I}_{\mathcal{C},n}(t) =& \frac{2\rho(\pi\lambda_{\mathcal{B}})^{1-\frac{\alpha}{2}}}{1-\exp(-\pi\lambda_{\mathcal{B}}R_F^2)}\cdot\gamma\left(1+\frac{\alpha}{2},\pi\lambda_{\mathcal{B}}R_F^2\right)\cdot\frac{r_{\hat{c},n}^{2-\nu}}{\nu-2} \\ &+ \rho r_{\hat{c},\hat{c}}^{\alpha} r_{\hat{c},n}^{-\nu}.\end{aligned} \tag{48}$$

D. Previous Interference Approximation (PIA)

In the PIA method, we assume that D2D receivers are capable of measuring the received interference power after the power allocation operation of D2D pairs in each time slot. In the initial time slot, the estimated mean aggregate interference based on the CGE method might be used. Then, each D2D receiver measures and records its received interference power in the current time slot and uses it to approximate the received interference power in the next time slot.

E. Comparison of Interference Estimation Methods

We compare the four interference estimation methods proposed in previous subsections. Firstly, the CGE method is most compatible with D2D pairs with simple hardware, but its performance depends sensitively on the radius of the guard zones and finding the best radius usually needs exhaustive search. Secondly, the AGE method requires each D2D receiver to measure the distances to its nearest CUE and its nearest interfering D2D transmitter. However, the AGE method can adaptively create guard zones and approximately estimate the two dominant interference components at a D2D receiver. Further, based on the AGE method, the EAGE method additionally requests the transmit power of the nearest CUE but accurately calculates the mean interference from the nearest CUE. Finally, the PIA method demands each D2D receiver to measure its received interference power in each time slot. Intuitively, when data queues and virtual power queues are strongly stable, the fluctuation of the received interference power of a D2D receiver is moderate. In this case, the received interference power in the previous time slot provides an appropriate approximation of the received interference power in the current time slot.

VII. Simulation and Comparison

In addition to the analytical results provided in Theorems 1 and 2, we further evaluate the performance of the proposed DIDA strategy through simulation in MATLAB.

A. Alternatives for Comparison

Note that the centralized algorithms proposed in [20]–[24] are based on a single-cell model and ignore inter-cell interference. Therefore, they cannot be directly applied to operate in multi-cell wireless networks or to satisfy the coverage probability guarantee of CUEs. Instead, the following two decentralized strategies are adopted for performance comparison.

*1) **Fixed strategy**:* Its flow control is the same as that of the proposed DIDA strategy. Then, each D2D transmitter deterministically consumes its individual interference budget (15) to transmit at a fixed power $P_f \triangleq (\frac{\ln U - \ln \beta}{S})^{\frac{\alpha}{2}}$ in each time slot.

*2) **On-Off strategy**:* Its flow control is the same as that of the proposed DIDA strategy. The on-off power allocation method in [16] selects the transmit power of each D2D pair from the decision set $\{0, P_{\max}\}$ solely based on its own CSI and a given threshold $g_{\min}$. The transmit probability of D2D pair n in time slot t is $\mathbb{P}_n(t) = \mathbb{P}[g_{n,n}(t) > g_{\min}] = e^{-g_{\min}}$. The definition of $g_{\min}$ in [16] aims to maximize the D2D transmission capacity without guaranteeing the CUE coverage probability. For the purpose of comparison, we need to modify the definition of $g_{\min}$ to meet the coverage probability guarantee of interior CUEs. Specifically, we define $g_{\min}$ as the optimal threshold maximizing the transmit probability $\mathbb{P}_n(t)$ while satisfying the individual interference budget (15), i.e.,

$$\limsup_{T\to\infty} \frac{1}{T}\sum_{t=0}^{T-1} \mathbb{E}_{P_n}\left[P_n(t)^{\frac{2}{\alpha}}\right] = \frac{P_{\max}^{\frac{2}{\alpha}}}{e^{g_{\min}}} = \frac{\ln U - \ln \beta}{S}, \quad (49)$$

resulting in $g_{\min} = \ln(\frac{SP_{\max}^{\frac{2}{\alpha}}}{\ln U - \ln \beta})$.

Note that the optimal flow control scheme used in the DIDA strategy is also optimal for the Fixed and On-Off strategies. This is because the flow control and power allocation decisions are decided by two independent problems $\mathbf{P}2$ and $\mathbf{P}3$.

B. Simulation Setup

We consider a two-tier network with multiple cells and D2D pairs, as illustrated in Fig. 1. The BSs, CUEs, and D2D transmitters are dropped based on independent PPPs of density $\lambda_{\mathcal{B}}$, $\lambda_{\mathcal{C}}$, and $\lambda_{\mathcal{D}}$ within a square of side-length 4000 m centered at the origin. Each BS $\mathbf{x}_i$ randomly selects an associated CUE within the interior circle $B(\mathbf{x}_i, R_F)$ as its interior CUE. In addition, each D2D receiver is uniformly located within a circle of radius $D_{\max}$ centered at its associated D2D transmitter. In order to remove the edge effect, we focus on the performance of interior CUEs and D2D transmitters inside the circle of radius 1000 m centered at the origin, and consider the CUEs and D2D transmitters outside the circle only for their effect on interference.

Default simulation parameters are shown in Table II. For simplicity of illustration, we focus on the bandwidth of one RB shared by all interior CUEs. For scenarios with higher bandwidth, similar results have been observed but are omitted to avoid redundancy. We set $\psi_n(x) = x, \forall n \in \Phi_{\mathcal{D}}$. We assume that the D2D arrival traffic amount follows uniform distribution with mean $\bar{A} = A_{\max}/2$. We consider 100 realizations of random point processes and 2000 time slots for each realization to evaluate the average performance. Simulation results are averaged both temporally and spatially after the stabilization of data queues and virtual power queues, i.e., for $t \in [1000, 2000]$. The guard radius set of the CGE method is $\{20\text{ m}, 60\text{ m}, 100\text{ m}, 140\text{ m}, 180\text{ m}, 220\text{ m}, 260\text{ m}, 300\text{ m}\}$.

TABLE II
DEFAULT SYSTEM PARAMETERS OF SIMULATION

Parameter	Symbol	Value
Density of BSs	$\lambda_{\mathcal{B}}$	4 BSs/km^2
Density of total CUEs	$\lambda_{\mathcal{C}}$	100 units/km^2
Density of D2D pairs reusing a RB	$\lambda_{\mathcal{D}}$	20 units/km^2
Radius of interior circle in FFR scheme	R_F	100 m
Noise power	σ^2	-174 dBm/Hz
Received signal power target of CUEs	ρ	-50 dBm
Maximum D2D per-RB transmit power	$P_{\max}$	10 mW
Maximum distance between a D2D pair	$D_{\max}$	80 m
Path-loss exponent for UE-to-BS channels	α	3.75
Path-loss exponent for UE-to-UE channels	ν	4
Spectrum bandwidth of a RB	w	180 kHz
Duration of a time slot	τ	1 ms
Maximum D2D arrival traffic amount	$A_{\max}$	1 kbit/slot
SINR threshold of CUEs	η	0 dB
Coverage probability threshold of CUEs	β	0.90

TABLE III
SUM-LOG UTILITY OF CUE COVERAGE PROBABILITY.

	$\exp(\frac{1}{T_2-T_1}\sum_{t=T_1}^{T_2-1}\ln \mathbb{P}(\text{SINR}_m(t) > \eta))$						
V	1	2	3	4	5	6	7
DIDA-EAGE	0.89	0.89	0.89	0.89	0.89	0.89	0.89
DIDA-AGE	0.89	0.89	0.89	0.89	0.89	0.89	0.89
DIDA-PIA	0.89	0.89	0.89	0.89	0.89	0.89	0.89
DIDA-CGE Best	0.89	0.89	0.89	0.89	0.88	0.88	0.88
DIDA-CGE Worst	0.89	0.89	0.89	0.89	0.89	0.89	0.89
Fixed	0.88	0.88	0.88	0.88	0.88	0.88	0.88
On-Off	0.89	0.89	0.89	0.89	0.89	0.89	0.89

C. Simulation Results

Table III shows the coverage probability guarantee of interior CUEs over time slots from $T_1 = 1000$ to $T_2 = 2000$ through transforming the sum-log utility in (7) to compare with the CUE coverage probability threshold $\beta = 0.9$. Given the default simulation parameters and the guard radius set of the CGE method, the best and worst guard radiuses of the DIDA-CGE strategy are 180 m and 20 m, respectively, which correspond to the labels DIDA-CGE Best and DIDA-CGE Worst. By stabilizing the virtual power queues (18) and satisfying the individual D2D interference budget (15) distributively, all strategies preserve the sum-log utility of CUE coverage probability near the overage probability threshold with a maximum gap of 0.02. This small gap is due to the slight overestimate of analytical formula (10) by assuming that the radius of interior circle is small enough. These results indicate that the satisfaction of the coverage probability constraint (7) can be transformed into the stabilization of the virtual power queue (18) in a distributed manner by using the proposed individual D2D interference budgeting method, and that the stabilization of virtual power queues does not depend on the accuracy of interference estimation in the proposed DIDA strategy.

Fig. 5 illustrates the average throughput of D2D pairs versus the control parameter, V. The DIDA strategy, based on any of the proposed interference-estimation methods, substantially outperforms the alternative strategies in throughput, which indicates that the DIDA strategy performs well even with a simple interference estimation method. In particular, the DIDA-EAGE and DIDA-AGE strategies achieve the highest D2D average throughput, which suggests that adaptive interference-

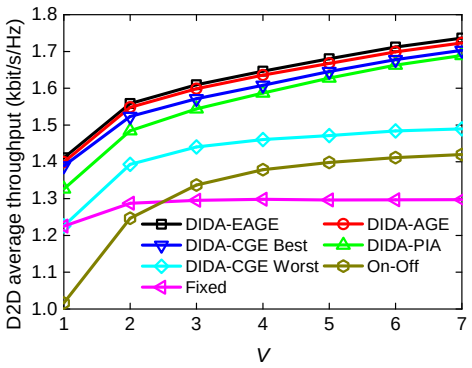

Fig. 5. D2D average throughput versus V.

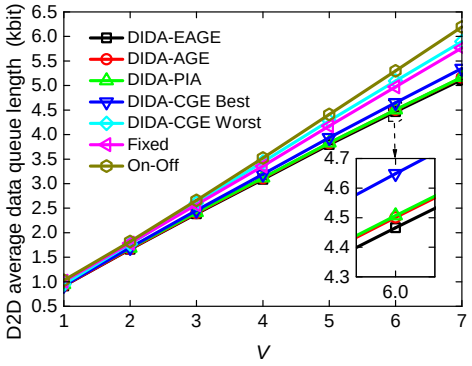

Fig. 6. D2D average data queue length versus V.

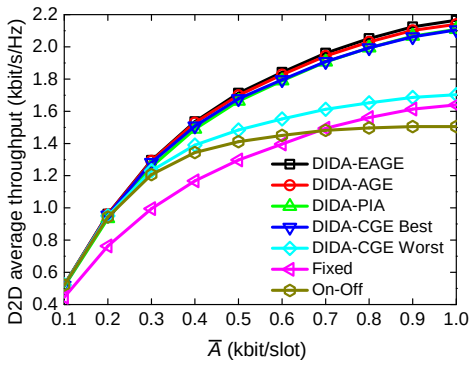

Fig. 7. D2D average throughput versus the D2D average traffic arrival amount.

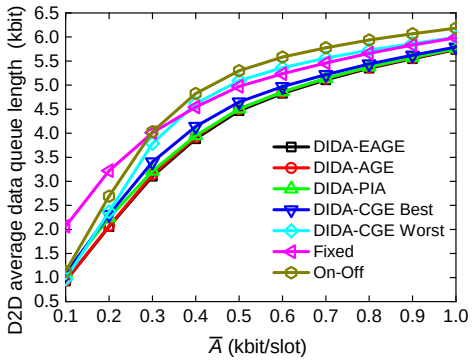

Fig. 8. D2D average data queue length versus the D2D average traffic arrival amount.

estimation methods are more attractive. This is because the EAGE and AGE methods can better estimate the dominant interference components of D2D receivers than the CGE and PIA methods, even without exhaustive search of guard radius. Although the best case of the DIDA-CGE strategy also obtains high throughput, the best guard radius varies sensitively with scenario parameters, and searching the best guard radius is difficult in practice. In addition, due to the strong stability of data queues and virtual power queues, the DIDA-PIA strategy can obtain high D2D average throughput. Moreover, compared with the Fixed strategy, the On-Off strategy accumulates the arrival traffic of D2D pairs and exploits favorable transmission opportunities because of its on-off switch. As a result, the performance of the On-Off strategy is more sensitive to V. Fig. 5 also shows that increasing V improves the average throughput of D2D pairs, which is consistent with Theorem 2.

Fig. 6 presents the average data queue length of D2D pairs versus V. We observe that the DIDA-EAGE strategy also achieves slightly better performance than other strategies using the same flow control scheme. Comparing the two alternative strategies, we observe that the On-Off strategy spends more time slots waiting for good channel qualities, while the Fixed strategy activates D2D transmitters in every time slot and achieves lower average D2D data queue length. In addition, the DIDA strategy based on the proposed interference-estimation methods jointly considers the local CSI and QSI of D2D pairs and dynamically controls the transmit power of D2D transmitters, which yields both higher average throughput and lower average data queue length. Also, Fig. 6 reveals that the average data queue length of D2D pairs increases with V, because increasing V equivalently admits more traffic into data queues as shown in (27). Together with Fig. 5, this illustrates the effect of the control parameter V in tuning the tradeoff between throughput and delay, which is expected for strategies that employ the Lyapunov optimization framework.

Setting $V = 6$ and varying the average arrival traffic amount of D2D pairs, the average throughput and average data queue length of D2D pairs versus the average D2D traffic arrival amount, $\bar{A}$, are shown in Fig. 7 and Fig. 8, respectively. Increasing the average arrival traffic amount improves the average throughput of D2D pairs because the time-average transmission amount of D2D pairs is better exploited. Furthermore, increasing the average arrival traffic amount enlarges the average data queue length of D2D pairs. Among all the strategies considered in this paper, the DIDA-EAGE strategy achieves the highest D2D average throughput and the lowest D2D average data queue length. In addition, the performance of the DIDA-AGE strategy is slightly better than that of the DIDA-CGE Best strategy and that of the DIDA-PIA strategy. Furthermore, comparing the DIDA-CGE Worst strategy and two alternative strategies, we observe that the DIDA-CGE Worst and On-Off strategies give superior performance in the region of low average arrival traffic amount, while the Fixed strategy performs better in the region of high average arrival traffic amount. These results can be explained by the Cumulative Distribution Function (CDF) of D2D transmission

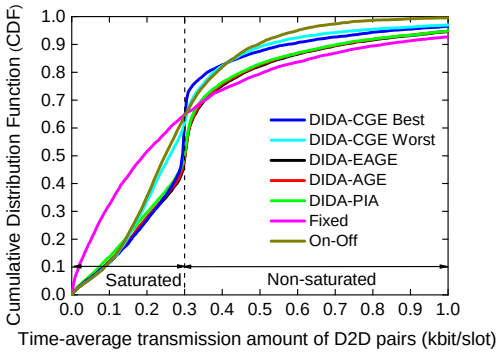

Fig. 9. CDF of D2D average transmission amount over one RB with $\bar{A} = 0.3$ kbit/slot.

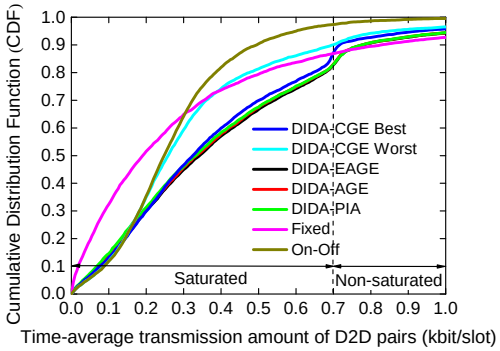

Fig. 10. CDF of D2D average transmission amount over one RB with $\bar{A} = 0.7$ kbit/slot.

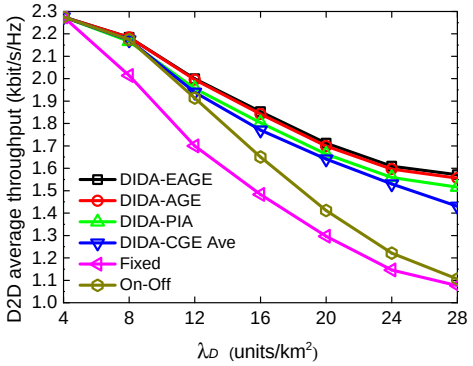

Fig. 11. D2D average throughput versus the density of D2D pairs.

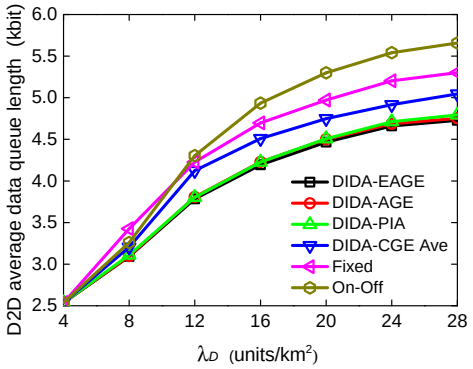

Fig. 12. D2D average data queue length versus the density of D2D pairs.

amount shown in Fig. 9 and Fig. 10.

Setting $V = 6$ and setting $\bar{A} = 0.3$ kbit/slot and 0.7 kbit/slot, respectively, Fig. 9 and Fig. 10 present the CDF of transmission amount for all D2D pairs in 100 network realizations. By considering the QSI of both data queues and virtual power queues, those DIDA strategies with proper interference estimation methods, e.g., EAGE, AGE, PIA, and the best case of CGE, push the distribution of D2D transmission amount towards their average arrival traffic amount $\bar{A}$. Treating the Fixed strategy as a baseline, we separate the D2D pairs into two categories, saturated D2D pairs and non-saturated D2D pairs. Specifically, under the Fixed strategy, a D2D pair is saturated if it achieves a time-average transmission amount lower than its average arrival traffic amount. Otherwise, the D2D pair is non-saturated. We observe that those DIDA strategies with proper interference estimation methods can significantly improve the transmission amount of the saturated D2D pairs and moderately reduce the transmission amount of the non-saturated D2D pairs. The latter is because these DIDA strategies can save the energy of the non-saturated D2D pairs and mitigate the interference from the non-saturated D2D pairs to other links when the data queue lengths of the non-saturated D2D pairs are relatively small. Accordingly, around the point of $\bar{R}_n = \bar{A}$, the CDF curves of those DIDA strategies with proper interference estimation methods sharply increase and generate intersections with the CDF curve of the Fixed strategy. In addition, comparing with the Fixed strategy, we observe that the DIDA-CGE Worst strategy and the On-Off strategy moderately enhance the performance of those D2D pairs having low transmission amount under the Fixed strategy, which explains the aforementioned phenomenon in Fig. 7 and Fig. 8.

Setting $V = 6$ and varying the density of D2D pairs, the average throughput and average data queue length of D2D pairs versus the density of D2D pairs, $\lambda_{\mathcal{D}}$, are shown in Fig. 11 and Fig. 12, respectively. The performance of the DIDA-CGE strategy is averaged over the set of its guard radius set. Increasing the density of D2D pairs does not only decrease the individual D2D interference budget (15) but also cause higher intra-tier and inter-tier interference, resulting in a decrease on the average performance of D2D pairs. When $\lambda_{\mathcal{D}} = 4$ $\mathrm{units/km}^2$, all D2D pairs are allowed to transmit with their maximum power in every time slot. As the density of D2D pairs rises and the individual D2D interference budget accordingly decreases, the transmit probability of D2D pairs using the On-Off strategy declines and the performance loss due to naive power allocation decisions increases. Consequently, the On-Off strategy works better than the Fixed strategy in the region of low D2D density, but its performance sharply declines as the D2D density increases. Although the On-Off strategy may perform well by adjusting $g_{\min}$ with respect to the density of D2D pairs, the value of the best $g_{\min}$ varies with the scenario parameters and searching for the best $g_{\min}$ is troublesome in practice. In contrast, by adaptively controlling the transmit power of D2D transmitters based on the local QSI and CSI of D2D pairs and the estimated received interference power at D2D receivers, the DIDA strategy can automatically choose a proper transmit power adjusting to

scenario parameters and obtain better performance than the Fixed and On-Off strategies.

VIII. Conclusions

In this paper, we investigate distributed delay-aware design for D2D communication underlaying multiple cells, to maximize the time-average throughput utility of each D2D pair while guaranteeing the queueing stability of D2D communication and the coverage probability requirement of interior CUEs. We derive the individual interference budget for each D2D pair to guarantee the coverage probability of interior CUEs and then propose a distributed interference-and-delay-aware flow control and power allocation strategy, along with four interference estimation methods. We also analytically derive the queue-length bound and throughput bound of D2D pairs under the DIDA strategy. The throughput performance of the proposed DIDA strategy with adaptive interference estimation is demonstrated through simulation and shown to exceed that of two known alternatives.

Appendix A
Proof of Theorem 1

Theorem 1 is proved based on the queueing laws (6) and (18), the upper-bound conditions (19)-(21), and the DIDA flow control and power allocation strategy in Algorithm 1.

Based on data queues (6), if $0 \le Q_n(t) \le V\psi'_{n,\max}$, then $Q_n(t+1) \le Q_n(t) + A_{\max} \le Q_{n,\max}$, $\forall n \in \Phi_{\mathcal{D}}$, $\forall t$. Further, if $V\psi'_{n,\max} < Q_n(t) \le Q_{n,\max}$, then $\gamma_n^*(t) = 0$ according to (27) and $Q_n(t+1) \le Q_n(t) \le Q_{n,\max}$. Since $Q_n(0) \le Q_{n,\max}$, we have $Q_n(t) \le Q_{n,\max}$, $\forall n \in \Phi_{\mathcal{D}}$, $\forall t$.

Let $H \triangleq \frac{\ln U - \ln \beta}{S}$. Based on virtual power queues (18), if $0 \le Z_n(t) \le Q_{n,\max} R_{\max} H^{-1}$, then $Z_n(t+1) \le Z_n(t) + P_{\max}^{\frac{2}{\alpha}} - H \le Z_{n,\max}$, $\forall n \in \Phi_{\mathcal{D}}$, $\forall t$. Suppose that $Q_{n,\max} R_{\max} H^{-1} < Z_n(t) \le Z_{n,\max}$. Assume that Algorithm 1 has an optimal power decision of $P_n^*(t) \ge H^{\frac{\alpha}{2}}$ in time slot t. Inserting $P_n^*(t) \ge H^{\frac{\alpha}{2}}$ into (26), we have

$$\begin{aligned} &Z_n(t) P_n^*(t)^{\frac{2}{\alpha}} - Q_n(t) R_n(\mathcal{P}^*(t), \mathcal{G}(t)) \\ &> Q_{n,\max} R_{\max} H^{-1} P_n^*(t)^{\frac{2}{\alpha}} - Q_{n,\max} R_{\max} \ge 0. \end{aligned} \tag{50}$$

Subsequently, (50) implies that $P_n^*(t) = 0$ is a better power decision than any $P_n^*(t) \ge H^{\frac{\alpha}{2}}$, which violates the assumption that $P_n^*(t) \ge H^{\frac{\alpha}{2}}$ is the optimal power decision. Hence, in time slot t, the power decision $P_n^*(t)$ should be less than $H^{\frac{\alpha}{2}}$ and $Z_n(t+1) \le Z_n(t) \le Z_{n,\max}, \forall n \in \Phi_{\mathcal{D}}, \forall t$. Finally, since $Z_n(0) \le Z_{n,\max}$, we have $Z_n(t) \le Z_{n,\max}$, $\forall n \in \Phi_{\mathcal{D}}$, $\forall t$.

Further, since V, $\psi'_{n,\max}$, $A_{\max}$, $R_{\max}$, and $P_{\max}$ are finite parameters, we have $\bar{Q}_n \le Q_{n,\max} < \infty$ and $\bar{Z}_n \le Z_{n,\max} < \infty, \forall n \in \Phi_{\mathcal{D}}$, such that the strong stability of queues (6) and (18) are satisfied based on [25, Definition 2.7]. Also, according to [25, Theorem 2.5], the D2D individual interference budget (15) is satisfied. Note that the proof above is irrelevant to the accuracy of interference estimation by D2D pairs.

Appendix B
Proof of Theorem 2

We restate the objective functions of problem $\mathbf{P3}$ and its approximated problem $\mathbf{P4}$ as

$$\begin{aligned} F(P_n(t)) =& Z_n(t) P_n(t)^{\frac{2}{\alpha}} \\ &- Q_n(t) w\tau \log_2\left(1 + \frac{P_n(t) r_{n,n}^{-\nu} g_{n,n}(t)}{I_n(t)}\right), \end{aligned} \tag{51}$$

$$\begin{aligned} \tilde{F}(P_n(t)) =& Z_n(t) P_n(t)^{\frac{2}{\alpha}} \\ &- Q_n(t) w\tau \log_2\left(1 + \frac{P_n(t) r_{n,n}^{-\nu} g_{n,n}(t)}{\mu_n(t) I_n(t)}\right). \end{aligned} \tag{52}$$

Let $P_n^*(t)$ and $\tilde{P}_n^*(t)$ be the optimal solutions of problems $\mathbf{P3}$ and $\mathbf{P4}$, respectively. We define the drift-plus-penalty gap in time slot t as

$$G = F(\tilde{P}_n^*(t)) - F(P_n^*(t)). \tag{53}$$

To prove Theorem 2, we first show the following lemma.

Lemma 1 $G \le (V\psi'_{n,\max} + A_{\max}) w\tau |\log_2 \mu_n(t)|, \quad \forall t.$

Proof: In order to prove Lemma 1, we separate the value of $\mu_n(t)$ into two regions: $0 < \mu_n(t) \le 1$ and $\mu_n(t) \ge 1$. Considering the case $0 < \mu_n(t) \le 1$, we can derive

$$F(P_n^*(t)) \ge \tilde{F}(P_n^*(t)) \ge \tilde{F}(\tilde{P}_n^*(t)), \tag{54}$$

where the former inequality follows from $0 < \mu_n(t) \le 1$ and the latter inequality follows from $\tilde{P}_n^*(t)$ being the optimal solution of problem $\mathbf{P4}$. Therefore,

$$\begin{aligned} G &= F(\tilde{P}_n^*(t)) - F(P_n^*(t)) \\ &\le F(\tilde{P}_n^*(t)) - \tilde{F}(\tilde{P}_n^*(t)) \\ &= Q_n(t) w\tau \log_2\left(\frac{1 + \frac{\tilde{P}_n^*(t) r_{n,n}^{-\nu} g_{n,n}(t)}{\mu_n(t) I_n(t)}}{1 + \frac{\tilde{P}_n^*(t) r_{n,n}^{-\nu} g_{n,n}(t)}{I_n(t)}}\right) \\ &\overset{(g)}{\le} Q_{\max} w\tau \log_2\left(\max\left\{1, \frac{1}{\mu_n(t)}\right\}\right) \\ &= (V\psi'_{n,\max} + A_{\max}) w\tau \log_2\left(\frac{1}{\mu_n(t)}\right), \end{aligned} \tag{55}$$

where (g) follows from $Q_n(t) \le Q_{\max}$ and the fact that $\frac{a+c}{b+d} \le \max\{\frac{a}{b}, \frac{c}{d}\}$, in which a, b, c, and d are arbitrary positive numbers and "=" holds if and only if $\frac{a}{b} = \frac{c}{d}$.

In addition, considering the case $\mu_n(t) \ge 1$, we can similarly obtain

$$F(\tilde{P}_n^*(t)) \le \tilde{F}(\tilde{P}_n^*(t)) \le \tilde{F}(P_n^*(t)). \tag{56}$$

As a result, the upper bound of G can be derived as

$$\begin{aligned} G &= F(\tilde{P}_n^*(t)) - F(P_n^*(t)) \\ &\le \tilde{F}(P_n^*(t)) - F(P_n^*(t)) \\ &= Q_n(t) w\tau \log_2\left(\frac{1 + \frac{P_n^*(t) r_{n,n}^{-\nu} g_{n,n}(t)}{I_n(t)}}{1 + \frac{P_n^*(t) r_{n,n}^{-\nu} g_{n,n}(t)}{\mu_n(t) I_n(t)}}\right) \\ &\le Q_{\max} w\tau \log_2\left(\max\left\{1, \mu_n(t)\right\}\right) \\ &= (V\psi'_{n,\max} + A_{\max}) w\tau \log_2 \mu_n(t). \end{aligned} \tag{57}$$

Combining (55) and (57) proves Lemma 1. ■

Further, using Lemma 1, the drift-plus-penalty function under the DIDA strategy is upper bounded by

$$\begin{aligned}&\Delta(\mathbf{\Theta}_n(t)) - V\mathbb{E}\{\psi_n(\gamma_n(t))|\mathbf{\Theta}_n(t)\}\\&\leq B + (V\psi'_{n,\max} + A_{\max})w\tau|\log_2\mu_n(t)|\\&- V\mathbb{E}\{\psi_n(\gamma_n^*(t))|\mathbf{\Theta}_n(t)\}\\&+ Q_n(t)\mathbb{E}\left\{\gamma_n^*(t) - R_n(P_n^*(t), I_n(t))|\mathbf{\Theta}_n(t)\right\}\\&+ Z_n(t)\mathbb{E}\Big\{P_n^*(t)^{\frac{2}{\alpha}} - \frac{\ln U - \ln\beta}{S}\Big|\mathbf{\Theta}_n(t)\Big\}, \forall n \in \Phi_{\mathcal{D}}.\end{aligned} \tag{58}$$

where $R_n(P_n^*(t), I_n(t))$ is the potential transmission amount of D2D pair n in time slot t under its recived interference $I_n(t)$ and the corresponding optimal solution $P_n^*(t)$. Then, based on [25, Theorem 4.8], we can directly derive Theorem 2. Details are omitted to avoid redundancy.

Appendix C
Lower Bound of Time-Average Mean Transmit Power of D2D Pairs

When the virtual power queues Z_n, $\forall n \in \Phi_{\mathcal{D}}$, are stable, each D2D pair individually solves problem $\mathbf{P4}$ using an approximated transmission amount and fully consumes its individual interference budget (15), yielding

$$\limsup_{T\to\infty}\frac{1}{T}\sum_{t=0}^{T-1}\mathbb{E}\left[P_n(t)^{\frac{2}{\alpha}}\right] = \frac{\ln U - \ln\beta}{S}. \tag{59}$$

Because $f(x) = x^{\frac{2}{\alpha}}$ is a concave function for $\alpha > 2$, applying Jensen's inequality yields

$$\begin{aligned}\limsup_{T\to\infty}\frac{1}{t}\sum_{t=0}^{T-1}\mathbb{E}[P_n(t)] &\geq \left(\limsup_{T\to\infty}\frac{1}{T}\sum_{t=0}^{T-1}\mathbb{E}\left[P_n(t)^{\frac{2}{\alpha}}\right]\right)^{\frac{\alpha}{2}}\\&= \left(\frac{\ln U - \ln\beta}{S}\right)^{\frac{\alpha}{2}}.\end{aligned} \tag{60}$$

References

[1] K. Doppler, M. Rinne, C. Wijting, C. Ribeiro, and K. Hugl, "Device-to-device communication as an underlay to LTE-advanced networks," *IEEE Commun. Mag.*, vol. 47, no. 12, pp. 42–49, Dec. 2009.

[2] G. Fodor, E. Dahlman, G. Mildh, S. Parkvall, N. Reider, G. Miklos, and Z. Turanyi, "Design aspects of network assisted device-to-device communications," *IEEE Commun. Mag.*, vol. 50, no. 3, pp. 170–177, Mar. 2012.

[3] L. Lei, Z. Zhong, C. Lin, and X. Shen, "Operator controlled device-to-device communications in LTE-advanced networks," *IEEE Wirel. Commun.*, vol. 19, no. 3, pp. 96–104, Jun. 2012.

[4] D. Feng, L. Lu, Y. Yuan-Wu, G. Li, S. Li, and G. Feng, "Device-to-device communications in cellular networks," *IEEE Commun. Mag.*, vol. 52, no. 4, pp. 49–55, Apr. 2014.

[5] X. Lin, J. Andrews, A. Ghosh, and R. Ratasuk, "An overview of 3GPP device-to-device proximity services," *IEEE Commun. Mag.*, vol. 52, no. 4, pp. 40–48, Apr. 2014.

[6] A. Ramezani-Kebrya, M. Dong, B. Liang, G. Boudreau, and S. H. Seyedmehdi, "Optimal power allocation in Device-to-Device communication with SIMO uplink beamforming," in *Proc. IEEE SPAWC*, Stockholm, Sweden, June 2015, pp. 425–429.

[7] R. AliHemmati, B. Liang, M. Dong, G. Boudreau, and S. H. Seyedmehdi, "Long-term power allocation for multi-channel device-to-device communication based on limited feedback information," in *Proc. ASILOMAR, Pacific Grove, California*, Nov. 2016, pp. 729–733.

[8] A. Ramezani-Kebrya, M. Dong, B. Liang, G. Boudreau, and S. H. Seyedmehdi, "Robust power optimization for Device-to-Device communication in a multi-cell network under partial CSI," in *Proc. IEEE ICC, Paris, France*, May 2017.

[9] C.-H. Yu, K. Doppler, C. Ribeiro, and O. Tirkkonen, "Resource sharing optimization for device-to-device communication underlaying cellular networks," *IEEE Trans. Wireless Commun.*, vol. 10, no. 8, pp. 2752–2763, Aug. 2011.

[10] P. Liu, C. Hu, T. Peng, R. Qian, and W. Wang, "Admission and power control for device-to-device links with quality of service protection in spectrum sharing hybrid network," in *Proc. IEEE PIMRC, Sydney, Australia*, Sept. 2012, pp. 1192–1197.

[11] F. Teng, D. Guo, M. Honig, W. Xiao, and J. Liu, "Power control based on interference pricing in hybrid D2D and cellular networks," in *Proc. IEEE Globecom Wkshps, Anaheim, USA*, Dec. 2012, pp. 676–680.

[12] R. Yin, C. Zhong, G. Yu, Z. Zhang, K. K. Wong, and X. Chen, "Joint spectrum and power allocation for D2D communications underlaying cellular networks," *IEEE Trans. Veh. Technol.*, vol. 65, no. 4, pp. 2182–2195, Apr. 2016.

[13] R. Yin, G. Yu, H. Zhang, Z. Zhang, and G. Li, "Pricing-based interference coordination for D2D communications in cellular networks," *IEEE Trans. Wireless Commun.*, vol. 14, no. 3, pp. 1519–1532, Mar. 2015.

[14] S. Kusaladharma, P. Herath, and C. Tellambura, "Underlay interference analysis of power control and receiver association schemes," *IEEE Trans. Veh. Technol.*, vol. 65, no. 11, pp. 8978–8991, Nov. 2016.

[15] H. ElSawy, E. Hossain, and M.-S. Alouini, "Analytical modeling of mode selection and power control for underlay D2D communication in cellular networks," *IEEE Trans. Commun.*, vol. 62, no. 11, pp. 4147–4161, Nov. 2014.

[16] N. Lee, X. Lin, J. Andrews, and R. Heath, "Power control for D2D underlaid cellular networks: Modeling, algorithms, and analysis," *IEEE J. Sel. Areas Commun.*, vol. 33, no. 1, pp. 1–13, Jan. 2015.

[17] Z. Chen and M. Kountouris, "Distributed SIR-aware opportunistic access control for D2D underlaid cellular networks," in *Proc. IEEE Globecom, Austin, USA*, Dec. 2014, pp. 1540–1545.

[18] E. Zihan, K. W. Choi, and D. I. Kim, "Distributed random access scheme for collision avoidance in cellular device-to-device communication," *IEEE Trans. Wireless Commun.*, vol. 14, no. 7, pp. 3571–3585, Jul. 2015.

[19] W. Wang and V. Lau, "Delay-aware cross-layer design for device-to-device communications in future cellular systems," *IEEE Commun. Mag.*, vol. 52, no. 6, pp. 133–139, Jun. 2014.

[20] X. Mi, M. Zhao, L. Xiao, S. Zhou, and J. Wang, "Delay-aware resource allocation and power control for device-to-device communications," in *Proc. IEEE WCNC Wkshps, New Orleans, USA*, Mar. 2015, pp. 311–316.

[21] L. Lei, Y. Kuang, N. Cheng, X. S. Shen, Z. Zhong, and C. Lin, "Delay-optimal dynamic mode selection and resource allocation in device-to-device communications - part I: Optimal policy," *IEEE Trans. Veh. Technol.*, vol. 65, no. 5, pp. 3474–3490, May 2016.

[22] L. Lei, Y. Kuang, N. Cheng, X. Shen, Z. Zhong, and C. Lin, "Delay-optimal dynamic mode selection and resource allocation in device-to-device communications - part II: Practical algorithm," *IEEE Trans. Veh. Technol.*, vol. 65, no. 5, pp. 3491–3505, May 2016.

[23] W. Wang, F. Zhang, and V. Lau, "Dynamic power control for delay-aware device-to-device communications," *IEEE J. Sel. Areas Commun.*, vol. 33, no. 1, pp. 14–27, Jan. 2015.

[24] M. Sheng, Y. Li, X. Wang, J. Li, and Y. Shi, "Energy efficiency and delay tradeoff in device-to-device communications underlaying cellular networks," *IEEE J. Sel. Areas Commun.*, vol. 34, no. 1, pp. 92–106, Jan. 2016.

[25] M. J. Neely, *Stochastic Network Optimization with Application to Communication and Queueing Systems*. Morgan & Claypool, 2010.

[26] S. Huang, B. Liang, and J. Li, "Distributed interference and delay aware design for D2D communication in cellular networks," in *Proc. IEEE Globecom Wkshps ET5G*, Washington, USA, Dec. 2016, pp. 1–7.

[27] G. Boudreau, J. Panicker, N. Guo, R. Chang, N. Wang, and S. Vrzic, "Interference coordination and cancellation for 4G networks," *IEEE Commun. Mag.*, vol. 47, no. 4, pp. 74–81, Apr. 2009.

[28] W. Bao and B. Liang, "Uplink interference analysis for two-tier cellular networks with diverse users under random spatial patterns," *IEEE Trans. Wireless Commun.*, vol. 14, no. 3, pp. 1252–1265, Mar. 2015.

[29] N. Islam, V. Elepe, J. Shaikh, and M. Fiedler, "In small chunks or all at once? User preferences of network delays in web browsing sessions," in *Proc. IEEE ICC, Sydney, Australia*, Jun. 2014, pp. 575–580.

[30] D. Stoyan, W. S. Kendall, J. Mecke, and L. Ruschendorf, *Stochastic geometry and its applications*. Wiley New York, 1987, vol. 2.

[31] J. Nightingale, Q. Wang, C. Grecos, and S. Goma, "Video adaptation for consumer devices: opportunities and challenges offered by new standards," *IEEE Commun. Mag.*, vol. 52, no. 12, pp. 157–163, Dec. 2014.

[32] D. P. Bertsekas, R. G. Gallager, and P. Humblet, *Data networks*. Prentice-Hall International New Jersey, 1992, vol. 2.
[33] M. Haenggi and R. K. Ganti, *Interference in large wireless networks*. Now Publishers Inc, 2009.
[34] A. Hasan and J. Andrews, "The guard zone in wireless Ad hoc networks," *IEEE Trans. Wireless Commun.*, vol. 6, no. 3, pp. 897–906, Mar. 2007.
[35] 3GPP TS 36.213 V14.0.0, "E-UTRA physical channels and modulation," 3GPP, Tech. Rep., Sep. 2016.

Sheng Huang received the B.E. degree in telecommunication engineering from Xidian University, Xian, China, in 2011, where he is currently pursuing the Ph.D. degree. From 2015 to 2016, he was a Visiting Student with the University of Toronto. His research interests are network optimization and performance analysis in wireless heterogeneous networks.

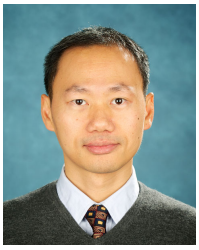

Ben Liang (S'94-M'01-SM'06) received honors-simultaneous B.Sc. and M.Sc. degrees in Electrical Engineering from Polytechnic University in Brooklyn, New York, in 1997 and the Ph.D. degree in Electrical Engineering with a minor in Computer Science from Cornell University in Ithaca, New York, in 2001. In the 2001 - 2002 academic year, he was a visiting lecturer and post-doctoral research associate with Cornell University. He joined the Department of Electrical and Computer Engineering at the University of Toronto in 2002, where he is currently a Professor. His research interests are in networked systems and mobile communications. He has served as an editor for the IEEE Transactions on Communications since 2014, and he was an editor for the IEEE Transactions on Wireless Communications from 2008 to 2013 and an associate editor for Wiley Security and Communication Networks from 2007 to 2016. He regularly serves on the organizational and technical committees of a number of conferences. He is a senior member of IEEE and a member of ACM and Tau Beta Pi.

Jiandong Li (M'96-SM'05) received the B.E., M.S., and Ph.D. degrees in communications and electronic system from Xidian University, Xian, China, in 1982, 1985, and 1991, respectively. He was a Visiting Professor with the Department of Electrical and Computer Engineering, Cornell University, from 2002 to 2003. He has been a faculty member of the school of Telecommunications Engineering at Xidian University since 1985, where he is currently a Professor at the State Key Laboratory of Integrated Service Networks Laboratory and also the Vice-President of Xidian University. His major research interests include wireless communication theory, cognitive radio and signal processing. He received the Distinguished Young Researcher from NSFC and Changjiang Scholar from Ministry of Education, China, respectively. He served as the General Vice Chair for ChinaCom 2009 and TPC Chair of IEEE ICCC 2013.